Muscle molecular adaptations to endurance exercise training are conditioned by glycogen availability: a proteomics-based analysis in the McArdle mouse model

Carmen Fiuza-Luces[1], Alejandro Santos-Lozano[2,3] (iD), Francisco Llavero[4], Rocío Campo[5] (iD), Gisela Nogales-Gadea[6,7] (iD), Jorge Díez-Bermejo[8], Carlos Baladrón[3], África González-Murillo[9], Joaquín Arenas[1], Miguel A. Martín[7] (iD), Antoni L. Andreu[7,10], Tomàs Pinós[7,10], Beatriz G. Gálvez[2,8] (iD), Juan A. López[5,11] (iD), Jesús Vázquez[5,11], José L. Zugaza[4,12,13] and Alejandro Lucia[2,8]

[1]Mitochondrial and Neuromuscular Diseases Laboratory and 'MITOLAB-CM', Research Institute of Hospital '12 de Octubre' ('i+12'), Madrid, Spain
[2]Research Institute of the Hospital 12 de Octubre ('i+12'), Madrid, Spain
[3]i+HeALTH, European University Miguel de Cervantes, Valladolid, Spain
[4]Achucarro – Basque Center for Neuroscience, Bilbao, Spain
[5]Laboratory of Cardiovascular Proteomics, Centro Nacional de Investigaciones Cardiovasculares Carlos III (CNIC), Madrid, Spain
[6]Research group in Neuromuscular and Neuropediatric Diseases, Neurosciences Department, Germans Trias i Pujol Research Institute and Campus Can Ruti, Autonomous University of Barcelona, Badalona, Spain
[7]Spanish Network for Biomedical Research in Rare Diseases (CIBERER), Spain
[8]Universidad Europea de Madrid, Madrid, Spain
[9]Fundación para la Investigación Biomédica, Hospital Universitario Niño Jesús and Instituto de Investigación Sanitaria La Princesa, Madrid, Spain
[10]Neuromuscular and Mitochondrial Pathology Department, Vall d'Hebron University Hospital, Research Institute (VHIR) Autonomous University of Barcelona, Barcelona, Spain
[11]Centro Integrado de Investigación Biomédica en Red en enfermedades cardiovasculares (CIBERCV), Madrid, Spain
[12]Department of Genetics, Physical Anthropology and Animal Physiology, Faculty of Science and Technology, University of the Basque Country, Leioa, Spain
[13]IKERBASQUE, Basque Foundation for Science, Bilbao, Spain

The Journal of Physiology

Key points

- Although they are unable to utilize muscle glycogen, McArdle mice adapt favourably to an individualized moderate-intensity endurance exercise training regime. Yet, they fail to reach the performance capacity of healthy mice with normal glycogen availability.
- There is a remarkable difference in the protein networks involved in muscle tissue adaptations to endurance exercise training in mice with and without glycogen availability.
- Indeed, endurance exercise training promoted the expression of only three proteins common to both McArdle and wild-type mice: LIMCH1, PARP1 and TIGD4.
- In turn, trained McArdle mice presented strong expression of mitogen-activated protein kinase 12 (MAPK12).

Abstract McArdle's disease is an inborn disorder of skeletal muscle glycogen metabolism that results in blockade of glycogen breakdown due to mutations in the myophosphorylase gene. We recently developed a mouse model carrying the homozygous p.R50X common human mutation (McArdle mouse), facilitating the study of how glycogen availability affects muscle molecular adaptations to endurance exercise training. Using quantitative differential analysis by liquid

chromatography with tandem mass spectrometry, we analysed the quadriceps muscle proteome of 16-week-old McArdle ($n = 5$) and wild-type (WT) ($n = 4$) mice previously subjected to 8 weeks' moderate-intensity treadmill training or to an equivalent control (no training) period. Protein networks enriched within the differentially expressed proteins with training in WT and McArdle mice were assessed by hypergeometric enrichment analysis. Whereas endurance exercise training improved the estimated maximal aerobic capacity of both WT and McArdle mice as compared with controls, it was $\sim$50% lower than normal in McArdle mice before and after training. We found a remarkable difference in the protein networks involved in muscle tissue adaptations induced by endurance exercise training with and without glycogen availability, and training induced the expression of only three proteins common to McArdle and WT mice: LIM and calponin homology domains-containing protein 1 (LIMCH1), poly (ADP-ribose) polymerase 1 (PARP1 – although the training effect was more marked in McArdle mice), and tigger transposable element derived 4 (TIGD4). Trained McArdle mice presented strong expression of mitogen-activated protein kinase 12 (MAPK12). Through an in-depth proteomic analysis, we provide mechanistic insight into how glycogen availability affects muscle protein signalling adaptations to endurance exercise training.

Introduction

The importance of endogenous muscle glycogen as a primary fuel source during exertion (particularly for intense endurance bouts) has been a fundamental concept in exercise physiology for half a century (Bergstrom *et al.* 1967; Pernow & Saltin, 1971). Accordingly, carbohydrate-rich diets have been traditionally recommended for athletes to ensure the replenishment of muscle glycogen stores to meet the metabolic demands of intense training exercise sessions and competitions (Bartlett *et al.* 2015). However, training with low muscle glycogen availability might induce some beneficial metabolic adaptations in the muscle tissue, including activation of key cell signalling kinases (e.g. protein kinase, AMP-activated, catalytic subunit α 1 and p38 mitogen-activated protein kinase (p38MAPK)), transcription factors (e.g. protein 53 (p53), peroxisome proliferator-activated receptor delta (PPARδ)) and transcriptional co-activators (e.g. peroxisome proliferator-activated receptor-1α (PGC-1α)) (Bartlett *et al.* 2015), increased fat oxidation (Lane *et al.* 2015), or delayed liver glycogenolysis (Webster *et al.* 2016). Elucidating the muscle metabolic adaptations to endurance exercise training as a function of glycogen availability is of interest as it may help to gain insight into the mechanisms that mediate the muscle adaptations to this type of training. This issue can be solved effectively by studying McArdle's disease because it allows the investigation of the effects of total unavailability of muscle glycogen on muscle adaptations to endurance exercise training without the need for dietary (e.g. extreme restrictions in carbohydrate intake) or pharmacological manipulations.

McArdle's disease (glycogen storage disease type V, OMIM® 232600) is the most prevalent disorder of muscle glycogen metabolism. This autosomal recessive disease is caused by pathogenic mutations (the most common of which is the stop codon mutation p.R50X) in both alleles of the *PYGM* gene (MIM#608455) encoding the skeletal-muscle isoform of glycogen phosphorylase, 'myophosphorylase', which leads to total deficiency of the enzyme (Santalla *et al.* 2014). Because myophosphorylase catalyses the breakdown of glycogen into glucose 1-phosphate in skeletal muscle fibres, patients are unable to obtain energy from their muscle glycogen stores (Santalla *et al.* 2014). This disorder provokes 'exercise intolerance' in virtually all affected individuals, which typically manifests in the form of acute crises of undue fatigue and muscle pain and stiffness since childhood (Lucia *et al.* 2012). Paradoxically, patients who are physically active are less severely affected than their inactive peers (Lucia *et al.* 2012). Prior non-controlled studies have reported benefits of supervised, moderate-intensity 'aerobic' exercise interventions (60–70% of maximum heart rate) for patients with McArdle's disease, in the form of increased peak oxygen uptake ($\dot{V}_{O_2\text{peak}}$) (Haller *et al.* 2006; Mate-Munoz *et al.* 2007) associated with improvements in the muscle levels of two key aerobic enzymes, citrate synthase and β-hydroxyacyl coenzyme A dehydrogenase (Haller *et al.* 2006). No other molecular data are, however, available on muscle tissue adaptations to training in these patients.

We recently generated a knock-in mouse model of McArdle's disease (mice homozygous for the *pygm p.R50X* mutation; Nogales-Gadea *et al.* 2012; Brull *et al.* 2015). Because this model closely mimics the phenotypes

observed in patients (Nogales-Gadea *et al.* 2012), it can serve as a useful tool to assess the effects of potential treatment interventions for McArdle's disease, including endurance exercise training. It was therefore the aim of our study to identify key proteins and pathways involved in the endurance exercise training adaptations at the muscle tissue level in McArdle's disease. To do this, we examined, using a controlled design, the effects of submaximal endurance training on the skeletal muscle proteome of wild-type (*wt/wt*) and McArdle (*p.R50x/p.R50x*) mice.

Methods

Ethical approval

The study received ethical institutional (Centre of Energy, Environment and Technical Research, CIEMAT) review board approval (reference number 179/15). Experiments were carried out according to the guidelines laid down by the institution's welfare committee, and conformed to the principles and regulations as described by Grundy (2015). All procedures were carried out according to European and Spanish legislative and regulatory guidelines (European convention ETS 123, on the use and protection of vertebrate mammals in experimentation and for other scientific purposes, and Spanish Law 32/2007, and R.D. 1201/2005 on the protection and use of animals in scientific research). The investigators of the present study understand the ethical principles under which *The Journal of Physiology* operates and our work complies with its animal ethics checklist. Whenever possible, efforts were made to minimize animal discomfort (see 'Endurance exercise training intervention in McArdle and wild-type mice').

Animals

Founder *p.R50X/p.R50X* knock-in mice of mixed genetic background (Nogales-Gadea *et al.* 2012) were back-crossed onto the wild-type CB7Bl/6J background for 10 generations. All the animals were genotyped with LoxP-F and LoxP-R as previously reported (Nogales-Gadea *et al.* 2012).

A total of 36 male mice (age: 8 weeks; wild-type: $n = 18$; McArdle: $n = 18$) were housed in Eurostandard type IIL microisolator cages (five mice maximum in each) under controlled conditions of temperature and humidity ($20 \pm 2°C$ and $55 \pm 10\%$, respectively) at the animal facility of the CIEMAT (registration no. ES280790000183, Madrid, Spain). The cages were lit (fluorescent lighting) from 07.00 to 19.00 h, and food (Harlan Teklad Global Diets 2914) and water (50 μm filtered and UV irradiated) were provided *ad libitum*.

Study design and endurance exercise training intervention

Pre-training phase. Mice were allowed to adapt to the treadmill (Harvard Apparatus; Panlab, Barcelona, Spain) in three sessions (on three separate days) as described (Fiuza-Luces *et al.* 2013); adaptation involved a gradual increase in running time, treadmill velocity and inclination, starting with placement of the mouse on the treadmill with movement at a very low speed during the first day (0% inclination and 0–5 cm s^{-1} speed for 1 min, with 0.1 mA electrical stimulation) and ending with a 20 min period at low running intensity on the third day (15% and 12 cm s^{-1}, electrical stimulation 0.1 mA, 1 Hz, 200 ms). A total of four treadmills were used and each mouse was consistently trained and tested on the same treadmill.

Maximal endurance exercise performance test. Once the mice had adapted to the treadmill, they were subjected to a gradual test until exhaustion to determine total running distance as a proxy of their maximal aerobic capacity (Hoydal *et al.* 2007). The test was performed after a warm-up period of 20 min at a speed of 12 cm s^{-1} (with 15% inclination), and followed a previous protocol from our group with slight modifications in workload increases (Fiuza-Luces *et al.* 2013). Thus, the initial velocity was 5 cm s^{-1}, and this was followed by workload increases of 3 cm s^{-1} every 2 min until exhaustion, while treadmill inclination was kept constant at 15% during the whole test and use of electrical stimulation (0.1 mA, 1 Hz, 200 ms). Mice were defined as exhausted when they spent more than 5 s continuously on the electric grid and were unable to continue running at the next speed (Ayala *et al.* 2009).

Group assignment. McArdle mice were paired-matched based on the total running distance they reached during the aforementioned test, and each pair was randomly assigned to an exercise ($n = 9$, subjected to an 8-week exercise training programme) or a control ('sedentary') group ($n = 9$, allowed to freely move in the cage, but did not perform the programme). The same method of group (exercise or control) assignment and number of animals per group was applied for wild-type mice.

Endurance exercise training intervention in McArdle and wild-type mice. Training load over a period of time is the result of the combination of frequency, duration and intensity of the different sessions. Thus, for the training loads of the two McArdle and wild-type exercise groups during the 8-week period to be comparable despite their different fitness level at baseline, we ensured that the weekly frequency of training sessions and the duration and relative intensity (the latter expressed as a percentage of the velocity reached at the end of the tests, V_{max}) of

each session was the same for the two groups. Thus, the intervention in both exercise groups included five weekly sessions (from Monday to Friday; session duration, 30–50 min), which was performed between 08.00 and 12.00 h. The duration and relative intensity of each session were also the same and increased gradually in the same manner in the two groups, beginning at low workloads in the first session (30 min at 50% of V_{max} and 0% gradient on the first day) and ending with 50 min at 70–75% of V_{max} and 15% gradient at the end of the programme (Fiuza-Luces *et al.* 2013). All the sessions included a warm-up period (15 min at 40% (start of the programme) to 50% of V_{max} (end)) and were followed by a cool-down period (5 min at 35% of V_{max}), both at the same treadmill slope used for the core part.

Whenever possible, efforts were made to minimize animal discomfort. Thus, only gentle tail touching was used to prompt the mice to run and no electrical stimulation was applied during the training sessions. In addition, because carbohydrate ingestion 30–40 min prior to exercise attenuates the risk of muscle damage in McArdle's disease (Lucia *et al.* 2008), for ethical reasons, during the hour before each session the McArdle mice were fed one Fruit Crunchies[TM] pellet (weight, 190 mg; 52% energy from carbohydrate, 20.2% protein, 11.5% fibre, 6.3% fat, 5.1% ash and <10% moisture) (Bio-Serv[TM], LBS Serving Biotechnology, UK). We verified that all exercise sessions started after the mice had eaten the pellet (which consistently took ≤60 min). Ingestion of pellets was chosen instead of parenteral administration of glucose to minimize animal discomfort. To ensure similar conditions in all groups, all the study mice also consumed the aforementioned pellet at the same time of the day.

Post-training phase. At the end of the endurance exercise training programme, all animals repeated the aforementioned performance test. Finally, 48 h after the last test, mice were killed by intraperitoneal injection with a lethal dose of Avertin (0.2%, 0.15 ml g^{-1}). We dissected the quadriceps muscles, trimmed of connective tissue, which were immediately snap-frozen in liquid nitrogen before storage at −80°C for proteomics analysis. We chose the quadriceps instead of other limb muscles (tibialis anterior, extensor digitorum longus, or soleus) based on its high glycolytic phenotype, for technical reasons (i.e. large size, allowing sufficient amount of sample for present and future investigations), and also for its use in recent research from our group aiming at identifying molecular markers of important cell functions (energy-sensing pathways, oxidative phosphorylation and autophagy/proteasome systems, oxidative damage, and sarcoplasmic reticulum Ca^{2+} handling) in McArdle mice (Fiuza-Luces *et al.* 2016).

Paired comparisons were made between the maximal distance measured before and after the training period

in the exercise and control group, in both McArdle and wild-type mice (Wilcoxon test). Analyses were performed with Stata statistical software (version 13, Stata Corp; College Station, TX, USA) for Mac. The statistical significance level was set at $P < 0.05$.

Proteomic analysis

Proteomic analysis was performed in 10 McArdle (5 per group) and 8 wild-type (4 per group) mice.

Sample preparation. Muscle samples were extracted in lysis buffer (2% SDS, 10 mM Tris(2-carboxyethyl) phosphine hydrochloride (TCEP) and 50 mM Tris–HCl, pH 7.5) by homogenizing the tissue with 3 cycles at 6500 rpm for 60 s each using a MagNA Lyser Instrument (Roche; Mannheim, Germany). Thereafter, samples were boiled for 5 min and incubated for 30 min at room temperature with agitation. Samples were centrifuged at 16,000 g for15 min, and protein concentration in the supernatant was determined with a Direct Detect IR spectrometer (Millipore Ibérica; Madrid, Spain).

Protein digestion and isobaric labelling. For the quantitative differential analysis by liquid chromatography with tandem mass spectrometry (LC-MS/MS) using isobaric tags (TMT 10-plex), ∼100 μg of total proteins was digested using the filter-aided protocol as previously described with minor modifications (Cardona *et al.* 2015). Proteins were diluted in 7 M urea and 0.1 mM Tris–HCl (pH 8.5) (UA) and loaded onto 10 kDa centrifugal filter devices (NanoSep 10k Omega, Pall Life Sciences; Port Washington, NY, USA). The buffer was replaced by washing filters with UA, and proteins were then alkylated using 50 mM iodoacetamide (IAA) in UA for 30 min in the dark. The excess of alkylating reagent was eliminated by washing three times with UA and three additional times with 50 mM ammonium bicarbonate. Proteins were digested overnight at 37°C with modified trypsin (Promega Biotech Ibérica; Alcobendas, Madrid, Spain) in 50 mM ammonium bicarbonate at 30:1 protein:trypsin (w/w) ratio. The resulting peptides were eluted by centrifugation with 50 mM ammonium bicarbonate (twice) and 0.5 M sodium chloride. Trifluoroacetic acid (TFA) was added to a final concentration of 1% and the peptides were desalted onto C18 Oasis-HLB cartridges (Waters; Milford, MA, USA) and dried-down for further analysis.

For stable isobaric labelling, the resulting tryptic peptides were dissolved in 100 mM tri-ethyl-ammonium bicarbonate (TEAB) buffer, and the peptide concentration was determined by measuring amide bonds with the Direct Detect system (Millipore Ibérica). Equal amounts of each peptide sample were labelled using 10-plex TMT Reagents (Thermo Fisher Scientific; Waltham, MA) according to

the manufacturer's protocol. Peptides were labelled with TMT reagents previously reconstituted with 70 μl of acetonitrile; after incubation at room temperature for 2 h, the reaction was stopped with 0.5% TFA, incubated for 30 min, and peptides were combined. Samples were concentrated in a Speed Vac, desalted onto C18 Oasis-HLB cartridges and dried-down for further analysis. To increase proteome coverage, TMT-labelled samples were fractionated by high-pH reverse phase chromatography (High pH Reversed-Phase Peptide Fractionation Kit, Pierce; Rockford, IL, USA) and concentrated as before.

Protein identification and quantification. Labelled peptides were analysed by LC-MS/MS using a C-18 reversed phase nano-column (75 μm I.D. × 50 cm, 2 μm particle size, Acclaim PepMap RSLC 100 C18; Thermo Fisher Scientific, Waltham, MA, USA) in a continuous acetonitrile gradient consisting of 0–30% B in 360 min and 50–90% B in 3 min (A = 0.1% formic acid; B = 90% acetonitrile, 0.1% formic acid). A flow rate of 200 nl min^{-1} was used to elute peptides from the nano-column to an emitter nanospray needle for real time ionization and peptide fragmentation on an Orbitrap Fusion mass spectrometer (Thermo Fisher Scientific). An enhanced FT-resolution spectrum (resolution = 70,000) followed by the MS/MS spectra from the *N*th most intense parent ions were analysed along the chromatographic run. Dynamic exclusion was set at 40 s.

For peptide identification, all spectra were analysed with Proteome Discoverer (version 2.1.0.81, Thermo Fisher Scientific) using SEQUEST-HT (Thermo Fisher Scientific). For database searching at the Uniprot database containing all sequences from mouse and contaminants (27April 2016; 48,644 entries), the parameters were selected as follows: trypsin digestion with two maximum missed cleavage sites, precursor and fragment mass tolerances of 2 Da and 0.02 Da, respectively, carbamidomethyl cysteine and TMT modifications at N-terminal and Lys residues as fixed modifications, and methionine oxidation as dynamic modification. Peptide identification was performed using the probability ratio method (Martinez-Bartolome *et al.* 2008) and false discovery rate (FDR) was calculated using inverted databases and the refined method (Navarro & Vazquez, 2009) with an additional filtering for precursor mass tolerance of 15 ppm (Bonzon-Kulichenko *et al.* 2015).

Identified peptides with an FDR equal to or lower than 1% FDR were used to quantify the relative abundance of each protein from reporter ion intensities, and statistical analysis of quantitative data was performed using the WSPP statistical model previously described (Navarro *et al.* 2014). In this model, protein log2-ratios are expressed as standardized variables; that is, in units of standard deviation (SD) according to their estimated variances (Z_q values).

Functional protein analysis. Functional protein analysis of the whole set of quantified proteins was performed using a novel algorithm system biology triangle (SBT), developed specifically for the analysis of coordinated protein responses in high-throughput quantitative proteomics experiments (Garcia-Marques *et al.* 2016). This algorithm correlates the performance of a group of proteins inside a category (biological process) in terms of their quantitative behaviour (relative abundance); thus, changes can be detected in functional biological processes far beyond individual protein responses. Variations in the abundance of annotated functional categories were visualized by comparing the cumulative frequency (sigmoid) plots of the standardized variable with that of the normal distribution, as in previous research (Isern *et al.* 2013). Individual protein changes were also considered for further analysis.

Determination of the differentially expressed proteins. The Kolmogorov–Smirnov test was applied to test if the data followed a normal distribution. Student's *t* test or the Wilcoxon rank-sum test was applied to identify differentially expressed proteins (i.e. 'proteins of interest') between exercise and control groups in both McArdle and wild-type mice. *P*-values were adjusted for multiple comparisons with FDR correction.

Biocomputational analysis of proteomics data

Processing of protein expression data. Murine proteins were converted into the corresponding human equivalent UniProt reviewed protein according to the following steps: (i) UniProt ID automatic crossing of the murine proteins with human proteome with corresponding databases (InParanoid (Sonnhammer & Ostlund, 2015) and the Mouse Genome Database (MGD; Blake *et al.* 2017)), (ii) gene name automatic crossing of the murine proteins with human proteome with corresponding databases (InParanoid; Turk *et al.* 1990) and (iii) Manual Blast (Altschul *et al.* 1990), selecting the best reviewed match presenting at least an identity value ≥ 70% and E-value ≤ 10^{-6}.

Molecular characterization of adaptation to endurance exercise training. Adaptation to endurance exercise training was characterized at the molecular level via manual curation of the literature. This characterization was performed in two steps: in the first step, we identified the main pathophysiological processes related to 'manifestative' adaptations in the skeletal muscle in response to endurance exercise training ('manifestative' signatures), which were further characterized at the protein level to provide a final list of 'condition effector' proteins (hereafter termed 'effectors') (Appendix,

Table A1). Hence, effectors are those proteins that, according to the existing literature, have previously been reported to play a critical role in the process of interest for a given study viz., skeletal muscle adaptations to endurance exercise training (databases: PubMed, ScienceDirect and Scopus; key words (and combinations thereof): protein, muscle, physical adaptations, sports, exercise, McArdle's disease and McArdle).

Contextualization of the differentially expressed proteins within 'adaptation to exercise training' protein network. Effector proteins were used to focus the analysis on the biological condition of interest in the human biological network. The direct interactions (physical interactions or functional relationships) among the differentially expressed proteins (in exercise *vs.* control groups), as well as the interactions between the differentially expressed proteins and the effectors of skeletal muscle adaptations to endurance exercise training, were assessed. Different publicly available databases were consulted for the human protein network generation (e.g. Reactome, Molecular INTeraction database (MINT) and BioGrid) (Herrando-Grabulosa *et al.* 2016; Iborra-Egea *et al.* 2017).

Mechanistic evaluation of the differentially expressed proteins in relation to endurance exercise training: artificial neuronal networks analysis. The possible molecular relationship between the differentially expressed proteins and skeletal muscle adaptations to endurance exercise training was evaluated by means of artificial neuronal networks (ANNs), following TPMS technology protocols (Herrando-Grabulosa *et al.* 2016; Iborra-Egea *et al.* 2017). This approach involves the generation of mathematical models of the biological processes through the use of artificial intelligence techniques. Then, mathematical models were solved by ANNs, which are supervised algorithms that identify relationships between the different nodes in the network. ANN analysis yields a score for each differential protein based on the validations of the prediction capacity of the mathematical models towards known drugs and diseases, as described in databases. The higher the score, the stronger is the predicted mechanistic relationship between the evaluated protein and the biological process. Each score is associated with a *P*-value that describes the probability of the result being a true positive one. Aiming to facilitate the understanding of the results, the obtained scores were divided into three categories: >76, strong ($P < 0.05$); 40–76, medium-strong ($P = 0.05$–0.25); and <40, weak ($P > 0.25$).

Proteins presenting 200+ interactions ('sticky proteins'), or proteins that do not have reported interactions, were not included in the topology as they may disrupt the correct assessment of existing relationships (Pache *et al.* 2008). Relationships between the differentially

expressed proteins and skeletal muscle adaptations to endurance exercise training were assessed both for individual proteins and for combinations of two proteins; thus, from all the reported protein interactions, the most interesting are those presenting a synergic effect. The synergy criteria were applied according to the approach described by Berenbaum (1989), in which a significant synergic effect is considered when the overall effect is >20% of the sum of the individual effects of the two proteins.

Visualization of the protein network. Cytoscape 3.5.1. software was used to study the representation of all the reported interactions (both from the significantly associated proteins and non-significantly associated proteins) according to the ANN score.

Enrichment analysis. The pathways and biological processes enriched within the differentially expressed proteins in the exercise and control groups within both McArdle and wild-type mice were assessed using a hypergeometric enrichment analysis approach (Rivals *et al.* 2007). Specifically, the enrichment was run over several sets of proteins, including: Gene Ontology (GO) terms (Biological Process, Cellular Component, Molecular Function) according to European Molecular Biology Laboratory (EMBL)–European Bioinformatics Institute (EBI)/UniProt-GO (The UniProt Consortium, 2017); pathways from the Kyoto Encyclopedia of Genes and Genomes (KEGG; Kanehisa *et al.* 2014), the Pharmacogenomics Knowledgebase (PharmGKB; Whirl-Carrillo *et al.* 2012) and the Small Molecule Pathway Database (SMPDB; Frolkis *et al.* 2010); pathological conditions, signatures and pathways from the Biological Effectors Database (BED; Iborra-Egea *et al.* 2017) and the regulatory molecular mechanisms included in Transcriptional Regulatory Relationships Unraveled by Sentence-based Text-mining (TRRUST) database (Han *et al.* 2015). Only those pathways that showed a statistically significant presence were presented (FDR *P*-value < 0.05).

Results

The training loads were common to both McArdle and wild-type exercise groups over the 8-week period and are shown in detail in Appendix, Table A2. The endurance exercise training programme was successful in inducing a significant improvement in the total running distance of both McArdle (141 (31 SD) m (pre-training) *vs.* 167 (48 SD) m (post-training); Wilcoxon test $P = 0.035$) and wild-type (275 (30 SD) *vs.* 353 (146 SD) m, $P = 0.041$) mice, whereas no significant change was found during the same time period in their sedentary controls (140 (41 SD) *vs.* 116 (48 SD) m, $P = 0.129$ for McArdle and 302 (85 SD) *vs.* 296 (103 SD) m,

$P = 0.726$ for wild-type mice). Although the relative improvement in total running distance did not differ between McArdle and wild-type mice (Mann–Whitney test, $P = 0.111$), the total running distance of McArdle mice was ~50% lower than that of wild-type mice both before and after the endurance exercise intervention. Individual data (total running distance) of the mice used for proteomic analyses are shown in Fig. 1. When expressed as V_{max}, the test results were as follows: McArdle, exercise group: 26 (3) cm s^{-1} (pre-training) *vs.* 29 (4) cm s^{-1} (post-training), Wilcoxon test $P = 0.054$; wild-type, exercise group: 36 (6) (pre-training) *vs.* 41 (8) cm s^{-1} (post-training), $P = 0.028$; McArdle, sedentary control group: 26 (4) *vs.* 24 (5) cm s^{-1}, $P = 0.123$; wild-type, sedentary control group: 38 (5) *vs.* 37 (7) cm s^{-1}, $P = 0.180$.

The body mass of the mice showed an increasing trend over time irrespective of genotype or intervention (exercise or control): (i) McArdle, exercise group: 20.8 (1.4) g (pre) and 22.0 (1.3) g (post), Wilcoxon test $P = 0.997$; (ii) McArdle, control group: 20.8 (1.3) g (pre) and 22.1 (0.81) g (post), $P = 0.031$; wild-type, exercise group: 18.7 (2.0) g (pre) and 21.3 (1.0) g (post), $P = 0.083$; wild-type, control group: 19.0 (1.9) g (pre) and 21.7 (2.1) g (post), $P = 0.805$.

Proteomics

Proteins of interest. Data provided by whole proteomic analysis regarding differential proteins within the sedentary and the trained groups of McArdle and wild-type mice, respectively, were analysed by applying Student's *t* test and the Wilcoxon rank-sum test. A total of 74 differentially expressed proteins between the trained and sedentary wild-type mice and 123 differentially expressed proteins between the trained and sedentary McArdle mice were found (Appendix, Table A3). Of these differentially expressed proteins in response to endurance exercise training, only three were common to wild-type and McArdle mice: LIM and calponin homology domains-containing protein 1 (LIMCH1); poly (ADP-ribose) polymerase 1 (PARP-1, also known as NAD$^+$ ADP-ribosyltransferase 1 or poly (ADP-ribose) synthase 1); and tigger transposable element derived 4 (TIGD4). Expression of all three proteins was higher in endurance exercise training than in untrained conditions, in both wild-type and McArdle mice; however, statistical significance was not reached for any after FDR adjustment.
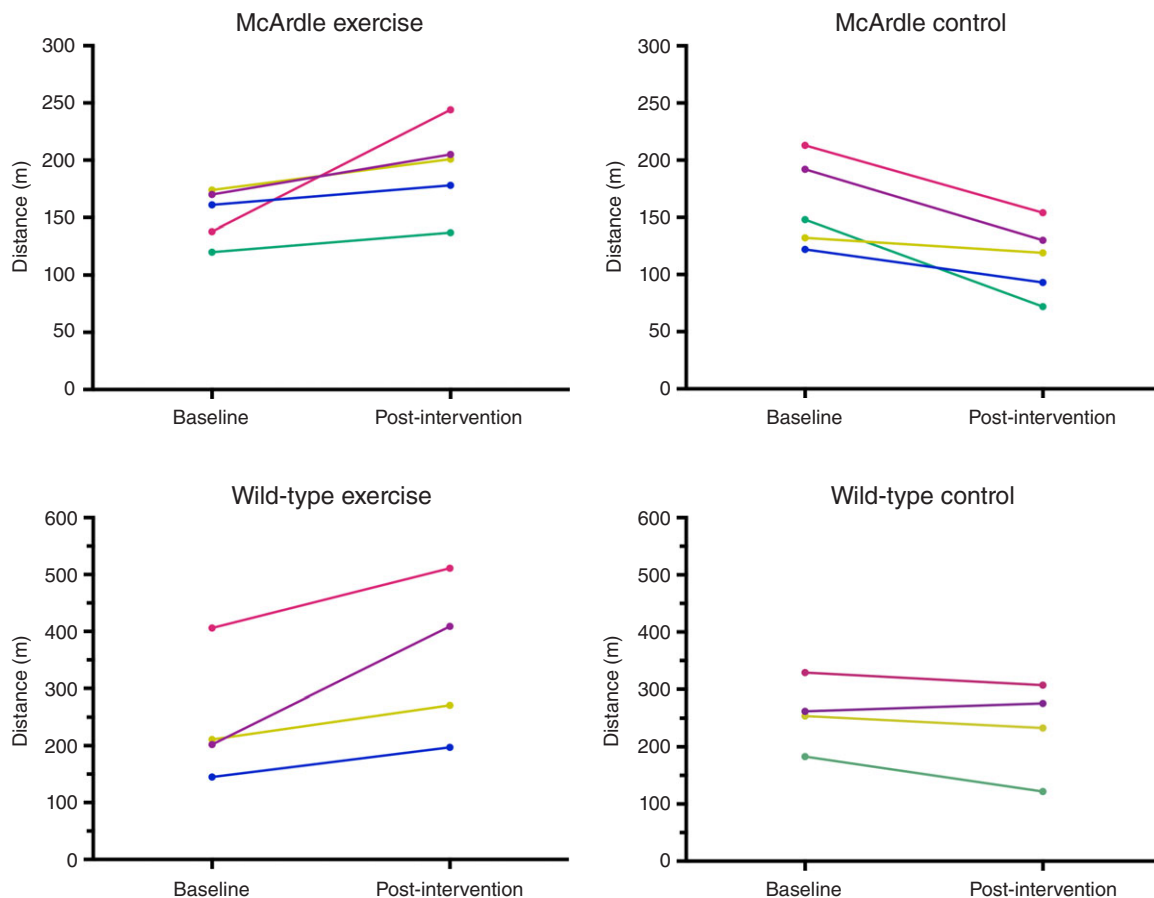

Figure 1. Individual responses during the intervention period in maximal distance during a gradual treadmill running test until exhaustion in mice used for proteomic analysis

Contextualization of the differentially expressed proteins within exercise training adaptation. The molecular characterization of the skeletal muscle adaptations to endurance exercise training was carried out through the review of specialized scientific literature. A total of 76 effector proteins were identified and classified into four groups according to their cellular function, such as adaptive muscle growth (14 proteins), muscle angiogenesis (8 proteins), glucose and lipid metabolism (12 proteins) and mitochondrial biogenesis and remodelling (48 proteins), with four of these 76 proteins belonging to two groups (angiogenesis + mitochondrial biogenesis and remodelling) at the same time, namely cyclic AMP-dependent transcription factor (ATF2), steroid hormone receptor ERR1 (ESRRA, or also ERRa), mitogen-activated protein kinase 12 (MAPK12) and myocyte-specific enhancer factor 2A (MEF2A, or MEF2), and one, PGC-1α, belonging to three groups (adaptive muscle growth + angiogenesis + mitochondrial biogenesis and remodelling) (Appendix, Table A1).

The role of the differentially expressed proteins in adaptation to endurance exercise training was evaluated according to the molecular characterization performed. The results of the analysis revealed that only one of the differentially expressed proteins in McArdle mice, MAPK12, had been previously related to skeletal muscle adaptations to exercise training (Table 1). MAPK12 is involved both in mitochondrial biogenesis and remodelling and muscle angiogenesis. By contrast, none of the differentially expressed proteins in wild-type mice has previously been reported to play a direct role in skeletal muscle adaptations to endurance exercise training (Table 2). However, while only one differentially expressed protein from the two lists (McArdle and wild-type mice) matches the effector proteins defined in the molecular characterization, it is remarkable that several of them interact with many effectors (Tables 1 and 2). In McArdle mice, ATP synthase H$^+$ transporting mitochondrial F1 complex γ polypeptide 1 (ATP5C1), MAPK12 and ATP synthase and H$^+$ transporting mitochondrial F1 complex ε subunit (ATP5E) were related to more than 10 effectors, and proteasome 26S subunit, non-ATPase 14 (PSMD14), integrin-linked kinase (ILK) and chaperonin containing TCP1 subunit 3 (CCT3) interacted with nine different effectors, while in wild-type mice, we found that poly(A) binding protein cytoplasmic 1 (PABPC1), protein kinase DNA-activated catalytic polypeptide (PRKDC), ribosomal protein lateral stalk subunit P0 (RPLP0), mitogen-activated protein kinase kinase 4 (MAP2K4) and protein kinase N1 (PKN1) interacted with more than 10 effectors, followed by ribosomal protein L21 (RLP21) interacting with up to nine different effectors. Additionally, the common differentially expressed protein between the two groups, PARP1, interacted with seven

different effectors, all of them involved in mitochondrial biogenesis and remodelling.

Mechanistic evaluation of the relationship with endurance exercise training: analysis of artificial neuronal networks. The potential molecular relationships between the differentially expressed proteins and skeletal muscle adaptations to endurance exercise training were evaluated through the analysis of mathematical models, to determine the possible activity relationships between protein sets or regions inside the network (i.e. ANN); this allowed us to provide a predictive score that quantifies the probability of the existence of a relationship between the evaluated differential proteins and network region (i.e. the different pathophysiological signatures characterized and adaptation to endurance exercise training as a whole). Each score is associated with a *P*-value that describes the probability of the result being a true positive result. To better understand the results, we divided the ranking score into four categories: strong ($P < 0.05$), medium-strong (P 0.05–0.25), weak ($P < 0.25$) and not assessed. As shown in Appendix, Table A4, it was not possible to evaluate 5 of 116 proteins for the McArdle mouse groups, and 5 of 73 for the wild-type groups. Nevertheless, the possible relationship between 111 proteins for McArdle mice and 68 proteins for wild-type mice was successfully assessed. When considering the differential proteins individually, ~28% and 22% of the proteins showed a significant relationship (strong or medium-strong category) with skeletal muscle adaptations to endurance exercise training in McArdle and wild-type mice, respectively. Moreover, when analysing the differential proteins in sets of two proteins, ~30% of the protein combinations showed a significant association with skeletal muscle adaptations to endurance exercise training, both in the McArdle and wild-type mice.

Relationships between the differentially expressed proteins and skeletal muscle adaptations to endurance exercise training: individual protein evaluation. As a result of the analysis of the relationship between individual proteins and skeletal muscle adaptations to endurance exercise training, a total of 33 proteins were reported to present a significant relationship with McArdle's disease mice and 16 with wild-type mice (Table 3). One of the differentially expressed proteins common to both mouse groups, PARP1, appeared to be significantly related to skeletal muscle adaptations to endurance exercise training. Moreover, the assessment of the potential relationship between the proteins of interest and skeletal muscle adaptations to endurance exercise training signatures allowed the evaluation of specific subsets of the physiological processes that in some cases were not detected by considering the whole context. For instance, nine proteins

Table 1. McArdle (*p.R50X/p.R50X*) mice: Summary of the interactions found between the differentially expressed proteins (in exercise *vs.* control groups) and of the protein effectors of skeletal muscle adaptations to endurance exercise training

UniProt	Gene name	Effectors	No. of interactions	No. of interactions with effectors	No. of interacting effectors, adaptive muscle growth	No. of interacting effectors, mitochondrial biogenesis & remodelling	No. of interacting effectors, glucose & lipid metabolism adaptations	No. of interacting effectors, angiogenesis
P36542	ATP5C1	✗	23	18	1	16	1	1
P53778	MAPK12	✓	19	15	4	12	0	3
P56381	ATP5E	✗	17	14	0	14	0	0
O00487	PSMD14	✗	18	9	2	4	3	0
Q13418	ILK	✗	17	9	1	7	1	1
P49368	CCT3	✗	12	9	3	5	1	1
P07237	P4HB	✗	11	8	0	6	2	1
O95831	AIFM1	✗	8	8	2	6	0	0
P46783	RPS10	✗	8	8	4	3	1	0
P09874	PARP1	✗	8	7	0	7	0	0
Q14204	DYNC1H1	✗	9	6	1	4	1	0
Q9BQG0	MYBBP1A	✗	9	6	3	3	1	1
P0C1S8	WEE2	✗	7	6	0	6	0	1
O43464	HTRA2	✗	6	6	0	6	0	1
P42704	LRPPRC	✗	6	6	4	3	0	1
P35232	PHB	✗	6	5	0	4	1	1
P25789	PSMA4	✗	6	3	0	2	1	0
Q96RQ3	MCCC1	✗	4	3	1	0	2	0
O43615	TIMM44	✗	4	3	0	2	1	0
Q99816	TSG101	✗	4	3	1	0	2	0
Q9HAV7	GRPEL1	✗	4	3	0	3	0	1
Q15119	PDK2	✗	3	3	0	0	3	0
P02647	APOA1	✗	8	2	0	1	1	0
P09936	UCHL1	✗	3	2	1	1	0	0
Q96K17	BTF3L4	✗	2	2	1	1	0	0
E9PAV3	NACA	✗	2	2	0	2	0	1
P61221	ABCE1	✗	2	2	1	1	0	0
P53985	SLC16A1	✗	2	2	0	2	0	0
P12694	BCKDHA	✗	2	2	0	0	2	0
O94973	AP2A2	✗	2	2	1	0	1	0
P07451	CA3	✗	2	2	0	0	2	0
P49257	LMAN1	✗	6	1	0	0	1	0
P02768	ALB	✗	6	1	0	1	0	0
Q06323	PSME1	✗	4	1	0	1	0	0
P84090	ERH	✗	4	1	0	1	0	0
P02671	FGA	✗	3	1	0	0	0	1
P01266	TG	✗	2	1	0	1	0	1

(Continued)

Table 1. Continued

UniProt	Gene name	Effectors	No. of interactions	No. of interactions with effectors	No. of interacting effectors, **adaptive muscle growth**	No. of interacting effectors, **mitochondrial biogenesis & remodelling**	No. of interacting effectors, **glucose & lipid metabolism adaptations**	No. of interacting effectors, angiogenesis
Q9UKY7	CDV3	✗	2	1	0	1	0	0
O95139	NDUFB6	✗	2	1	0	1	0	0
P02461	COL3A1	✗	2	1	0	0	0	1
O15357	INPPL1	✗	2	1	0	0	1	0
Q9BYN8	MRPS26	✗	2	1	0	0	1	0
Q9UKV0	HDAC9	✗	2	1	0	1	0	1
P13473	LAMP2	✗	2	1	0	0	1	0
P31146	CORO1A	✗	1	1	0	0	0	1
Q09666	AHNAK	✗	1	1	0	1	0	1
P13796	LCP1	✗	1	1	0	1	0	0
P21266	GSTM3	✗	1	1	0	0	1	0
Q96HC4	PDLIM5	✗	1	1	0	0	1	0
P17568	NDUFB7	✗	1	1	0	1	0	0
O43488	AKR7A2	✗	1	1	1	0	0	0
O60911	CTSV	✗	1	1	0	0	1	0
O75794	CDC123	✗	1	1	1	0	0	0
Q13884	SNTB1	✗	1	1	0	1	0	1

Symbols: non-effectors (×) and effectors (√) of skeletal muscle adaptations to endurance exercise training among the differentially expressed proteins.

of interest in McArdle mice and five in wild-type mice that were predicted to be related to at least one of the signatures of skeletal muscle adaptations to endurance exercise training were actually not found to be related to the general characterization of skeletal muscle adaptations to endurance exercise training (Table 3).

Relationships between the differentially expressed proteins and skeletal muscle adaptations to endurance exercise training: association in combination of two proteins. As a result of the analysis of the relationship between combinations of two proteins and skeletal muscle adaptations to endurance exercise training (Appendix, Table A4), a total of 2035 protein combinations were reported to present a significant relationship in McArdle mice and 719 in wild-type mice. When considering only the combinations with a significant synergic effect (synergic effect is considered when the overall effect is >20% of the amount of the individual effect of the two proteins), a total of 199 and 57 protein combinations were found for McArdle and wild-type mice, respectively. One of the common differentially expressed proteins in both groups, LIMCH1, appeared to be significantly related to

skeletal muscle adaptations to endurance exercise training in combination with other proteins.

In order to represent the intermolecular relationships obtained regarding protein interactions (Tables 1 and 2 and Appendix, Table A1) and mechanistic evaluation (Appendix, Table A4), a visual protein interaction network map was generated for both McArdle (Fig. 2) and wild-type (Fig. 3) mice. Only the proteins with a significant relationship with skeletal muscle adaptations to endurance exercise training (based on ANNs score) and their direct interactions appear on the representations. However, closer analysis of the signalling networks revealed that PARP1 was more profoundly overexpressed in trained McArdle than in trained wild-type mice (Figs 2 and 3, respectively).

Enrichment analysis. To analyse the expression data related to signalling pathways and clinical conditions, we undertook a hypergeometric enrichment analysis approach within the differentially expressed proteins in the trained and the control groups of McArdle and wild-type mice. As shown in Appendix, Table A5, 121 and 79 protein sets were found enriched in the comparison

Table 2. Wild-type (*wt/wt*) mice: summary of the interactions found between the differentially expressed proteins (in exercise *vs.* control groups) and of the protein effectors of skeletal muscle adaptations to endurance exercise training

UniProt	Gene name	Effectors	No. of Interactions	No. of interactions with effectors	No. of interacting effectors, **adaptive muscle growth**	No. of interacting effectors, **mitochondrial biogenesis & remodelling**	No. of interacting effectors, **glucose & lipid metabolism adaptations**	No. of interacting effectors, angiogenesis
P05388	RPLP0	✕	15	13	5	7	1	0
P11940	PABPC1	✕	18	12	5	6	1	0
P78527	PRKDC	✕	16	12	3	9	0	1
P45985	MAP2K4	✕	14	11	2	9	0	1
Q16512	PKN1	✕	14	11	3	8	0	1
P46778	RPL21	✕	10	9	5	4	0	0
P62879	GNB2	✕	9	8	1	6	1	3
Q562R1	ACTBL2	✕	8	8	1	7	0	0
P09874	PARP1	✕	9	7	0	7	0	0
P15056	BRAF	✕	9	7	1	6	0	1
P35544	FAU	✕	10	6	4	2	0	0
P42677	RPS27	✕	11	5	4	0	1	0
P16520	GNB3	✕	6	5	1	4	0	1
P56192	MARS	✕	6	5	1	4	0	0
P08195	SLC3A2	✕	5	5	1	3	1	1
P06737	PYGL	✕	5	4	1	2	1	0
P62140	PPP1CB	✕	6	3	0	1	2	1
O76094	SRP72	✕	6	2	1	0	1	0
Q99972	MYOC	✕	4	2	0	0	2	0
Q13683	ITGA7	✕	2	2	0	0	1	1
Q6PKG0	LARP1	✕	2	2	0	2	0	0
O75815	BCAR3	✕	4	1	0	1	0	0
P07951	TPM2	✕	2	1	0	0	1	0
P26012	ITGB8	✕	2	1	0	0	0	1
Q13409	DYNC1I2	✕	2	1	0	0	1	0
Q15631	TSN	✕	2	1	0	1	0	0
O95302	FKBP9	✕	1	1	0	0	1	0
P07108	DBI	✕	1	1	0	1	0	0
Q13564	NAE1	✕	1	1	0	1	0	0
Q13936	CACNA1C	✕	1	1	0	1	0	0
Q5VZF2	MBNL2	✕	1	1	0	0	1	0
Q5XPI4	RNF123	✕	1	1	0	1	0	0
Q8WUD1	RAB2B	✕	1	1	0	1	0	1
Q9HA65	TBC1D17	✕	1	1	0	1	0	0

Symbol: ×, non-effectors of skeletal muscle adaptations to exercise training among the differentially expressed proteins.

of control *vs.* exercise groups, both in McArdle and in wild-type mice. Subsequently, a pathway comparison between the results obtained from both conditions was performed, obtaining four common pathways and 117 and 75 proteins specifically enriched in McArdle and wild-type groups, respectively. The enriched protein sets common to McArdle and wild-type conditions corresponded to those related to high blood glucose levels and gene expression (BEDVES database: induction of oxidative stress diabetic neuropathies and induction of

Table 3. Differentially expressed proteins significantly linked to skeletal muscle adaptations in McArdle and wild-type mice

	McArdle (p.R50X/p.R50X) mice					Gene name	Wild-type (wt)/wt mice				
Gene name	Skeletal muscle adaptations to exercise	Adaptive muscle growth	Glucose & lipid metabolism adaptations	Muscle angiogenesis	Mitochondrial biogenesis and remodeling		Skeletal muscle adaptations to exercise	Adaptive muscle growth	Glucose & lipid metabolism adaptations	Muscle angiogenesis	Mitochondrial biogenesis and remodeling
APOA1	88%	5%	68%	17%	65 %	LARP1	72%	13%	15%	16%	14 %
MAPK12	84%	52%	5%	64%	92 %	DYNC1I2	71%	5%	10%	16%	52 %
CDV3	77%	16%	14%	6%	74 %	PARP1	71%	37%	19%	27%	71 %
LRPPRC	77%	70%	5%	67%	37 %	BRAF	70%	5%	13%	62%	65 %
TSG101	75%	61%	5%	11%	58 %	GNB2	69%	27%	70%	55%	70 %
ERH	72%	5%	14%	11%	54 %	INCENP	67%	5%	5%	5%	23 %
PARP1	71%	37%	19%	27%	71 %	CUTA	63%	5%	12%	16%	16 %
CAPN2	71%	5%	17%	5%	67 %	UBE2V2	63%	5%	5%	16%	11 %
CORO1A	71%	5%	5%	64%	49 %	GNB3	57%	12%	5%	68%	64 %
DYNC1H1	71%	33%	5%	24%	31 %	MYOC	57%	5%	68%	5%	5 %
PDK2	71%	5%	64%	18%	14 %	CACNA1C	54%	13%	15%	17%	65 %
CA3	71%	15%	66%	18%	5 %	ASB15	53%	6%	5%	16%	64 %
PHB	70%	8%	5%	5%	26 %	PPP1CB	48%	17%	5%	65%	18 %
TF	70%	6%	5%	16%	15 %	APOH	44%	6%	16%	5%	25 %
AIFM1	70%	5%	8%	5%	14 %	NAE1	43%	5%	7%	16%	5 %
HTRA2	69%	18%	5%	16%	48 %	MYH11	41%	15%	7%	5%	5 %
PSMD14	68%	6%	6%	6%	58 %	TSN	29%	15%	16%	16%	44 %
B2M	67%	7%	5%	11%	14 %	RPL21	22%	59%	6%	16%	5 %

(Continued)

Table 3. Continued

McArdle (p.R50X/p.R50X) mice

Gene name	Skeletal muscle adaptations to exercise	Adaptive muscle growth	Glucose & lipid metabolism adaptations	Muscle angiogenesis	Mitochondrial biogenesis and remodeling
ALB	65%	9%	8%	11%	48 %
SERPINA1	65%	5%	5%	5%	48 %
GSTM3	64%	5%	6%	16%	40 %
HDAC9	64%	6%	6%	69%	38 %
AK6	63%	6%	5%	16%	13 %
MYBBP1A	61%	69%	5%	66%	26 %
FGA	61%	6%	10%	16%	5 %
AP2A2	55%	32%	16%	11%	5 %
PSAP	54%	5%	8%	6%	5 %
P4HB	53%	15%	5%	16%	55 %
CCT3	48%	28%	5%	11%	65 %
UCHL1	45%	16%	5%	16%	40 %
ATP5C1	44%	5%	5%	5%	55 %
ATP5E	42%	5%	13%	10%	53 %
LMAN1	42%	5%	5%	16%	5 %
NDUFB7	39%	5%	16%	7%	47 %
PSMA4	35%	6%	17%	18%	51 %
NDUFB6	30%	6%	16%	11%	48 %
SEC13	28%	6%	8%	5%	62 %
MTM1	25%	23%	5%	10%	59 %
IGKC	23%	9%	5%	19%	57 %
LAMA5	22%	16%	15%	7%	50 %
RPS10	19%	59%	8%	16%	18 %
TUBAL3	18%	5%	7%	16%	64 %

Wild-type (*wt*)/*wt* mice

Gene name	Skeletal muscle adaptations to exercise	Adaptive muscle growth	Glucose & lipid metabolism adaptations	Muscle angiogenesis	Mitochondrial biogenesis and remodeling
FAU	19%	60%	6%	16%	48 %
RPLP0	17%	56%	5%	16%	34 %
SRP72	17%	36%	67%	5%	50%

The higher the artificial neuronal network (ANN) predictive score, the stronger is the relationship between the protein and skeletal muscle adaptations to endurance exercise training or its motives. ☐ ANN score (strong relationship) > 76% *P*-value < 0.05   ☐ ANN score 40–76 (strong-medium) *P*-value 0.05–0.25   ☐ ANN score (weak) < 40% *P*-value < 0.25.

oxidative stress diabetic neuropathies and retinopathies; GOFUNTION database: term poly(A) RNA binding and the GOLOCATION referring to cytosol).

The enriched protein sets reported within the differentially expressed proteins in exercise *vs.* control McArdle mice (Appendix, Table A5) reflect changes related to muscular adaptations to endurance exercise training that may be related to improvement in exercise tolerance, as well as to processes associated with the pathophysiology of the condition. Regarding enriched protein sets related to muscular adaptations to endurance exercise training, there were several pathways referring to mitochondria and their functions (Appendix, Table A6), including GO location terms referring to several mitochondrial structures such as the proton-transporting ATP synthase complex (responsible for ATP synthesis), and GO processes such as the respiratory electron transport chain. Furthermore, several pathways and GO terms related to lipid and protein metabolism are also reported in Appendix, Table A6, and enriched protein sets related to muscle structure and growth are described in Appendix, Table A7.

Conversely, the enriched protein sets within the wild-type groups were mainly related to endurance exercise training-induced physiological changes due to focal adhesion, actin cytoskeleton reorganization and phosphatidylinositol 3-kinase (PI3K) signalling pathway involvement (Appendix, Table A8). Moreover, several pathways referring to *β*-blocker activity also appeared to be enriched, possibly due to changes in catecholamine modulation (Appendix, Table A9).

Discussion

Although McArdle's*pt* disease causes 'exercise intolerance' (Lucia *et al.* 2012), under carefully controlled conditions, McArdle's patients may perform acute exercise safely, especially if carbohydrate solutions are taken before exercise to bypass the metabolic blockade that occurs upstream of the uptake of glucose by muscle fibres (Vissing & Haller, 2003). They may also adapt favourably to moderate-intensity endurance exercise training
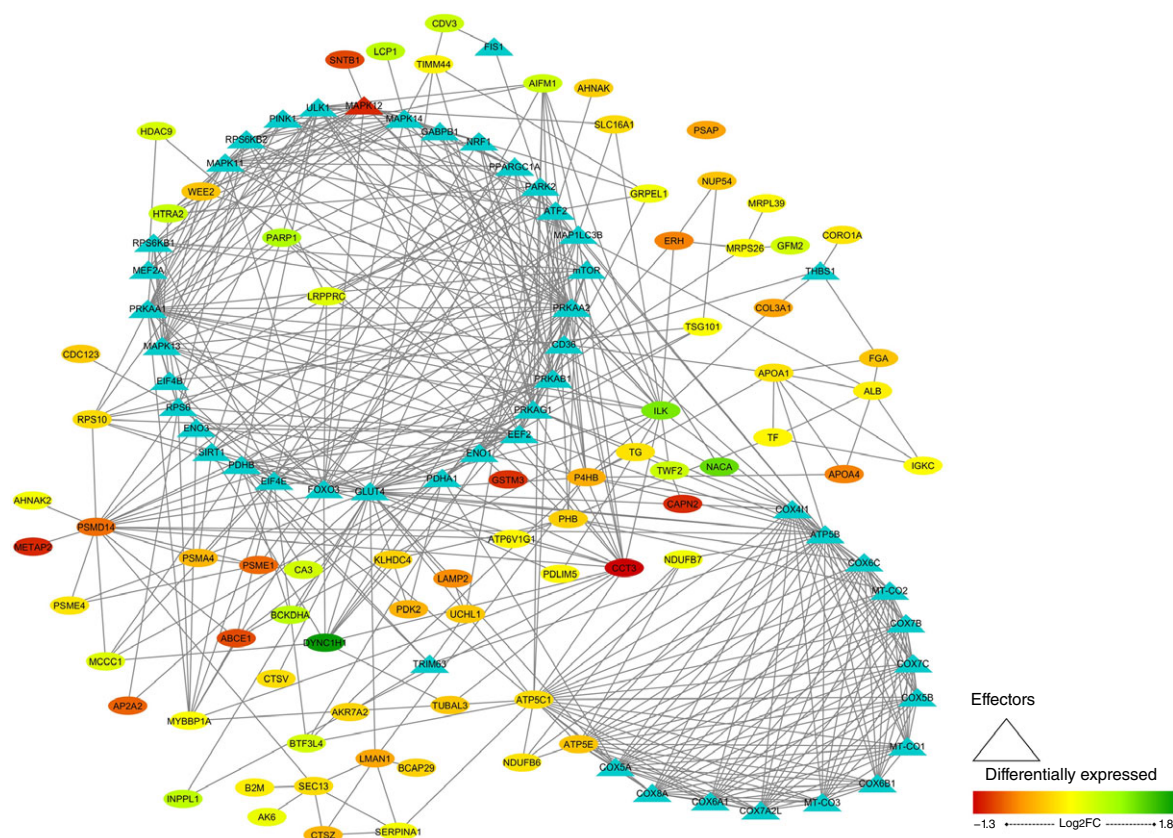

Figure 2. Visual protein interaction network of the proteins significantly related to skeletal muscle adaptations to endurance exercise training according to the artificial neuronal network score (ANNs), and their interacting proteins, in McArdle (*p.R50X/p.R50X*) mice

The network includes three representations of the following interactions: (i) within the differentially expressed proteins (ovals), (ii) between the differentially expressed proteins and skeletal muscle adaptions to endurance exercise effectors (ovals and triangles), and (iii) within the skeletal muscle adaptations to endurance exercise effectors (triangles). Note: all the *interactions*, from both the significantly associated proteins and the non-significantly associated proteins according to the ANN score, are reported.

(Haller *et al.* 2006; Mate-Munoz *et al.* 2007). Yet, no study has assessed in depth the molecular signals associated with muscle exercise adaptations in McArdle's patients and how they compare with those of healthy individuals. Accordingly, in the present study we aimed to identify, with no *a priori* hypothesis, the key proteins and protein networks linked to the effects of moderate-intensity endurance exercise training in a mouse model that closely mimics the phenotype of McArdle's patients (Nogales-Gadea *et al.* 2012). Unravelling the muscle metabolic adaptations to endurance exercise training with no muscle glycogen availability might help to gain insight into the proteome profile that characterizes muscle adaptations to such a type of training. This is an important question given that the skeletal muscle contains 50–75% of all the body proteins and is responsible for 30–50% of the whole body protein translation process (Frontera & Ochala, 2015). The majority of proteins identified here both in McArdle and wild-type mice control the expression of myriad genes related to angiogenesis, carbohydrate, lipid and protein metabolism, mitochondrial biogenesis and remodelling, and muscle growth.

In addition to reporting the first non-pharmacological intervention in this mouse model, a novel finding of our study was that, like patients, McArdle mice adapt favourably to an individualized moderate-intensity endurance exercise training regimen (albeit without reaching the performance capacity of healthy mice). Yet, our results revealed a remarkable difference in the protein networks involved in the muscle tissue adaptations that occur with endurance exercise training with normal glycogen availability (wild-type mice) as compared with those that occur in conditions of blocked glycogenolysis (McArdle mice). Indeed, endurance exercise training promoted the expression of only three proteins common to both McArdle and wild-type mice: LIMCH1, PARP1 and TIGD4. Likely, all three proteins play a prominent role in the relationship between skeletal muscle plasticity and endurance exercise training, independent of muscle glycogen availability, which warrants further investigation. It is well known that during exercise, numerous stress signals are transduced to activate intracellular signalling pathways controlling skeletal muscle gene transcription and translation (Bassel-Duby & Olson, 2006; Koulmann & Bigard, 2006; Favier *et al.* 2008; Russell, 2010). Against this
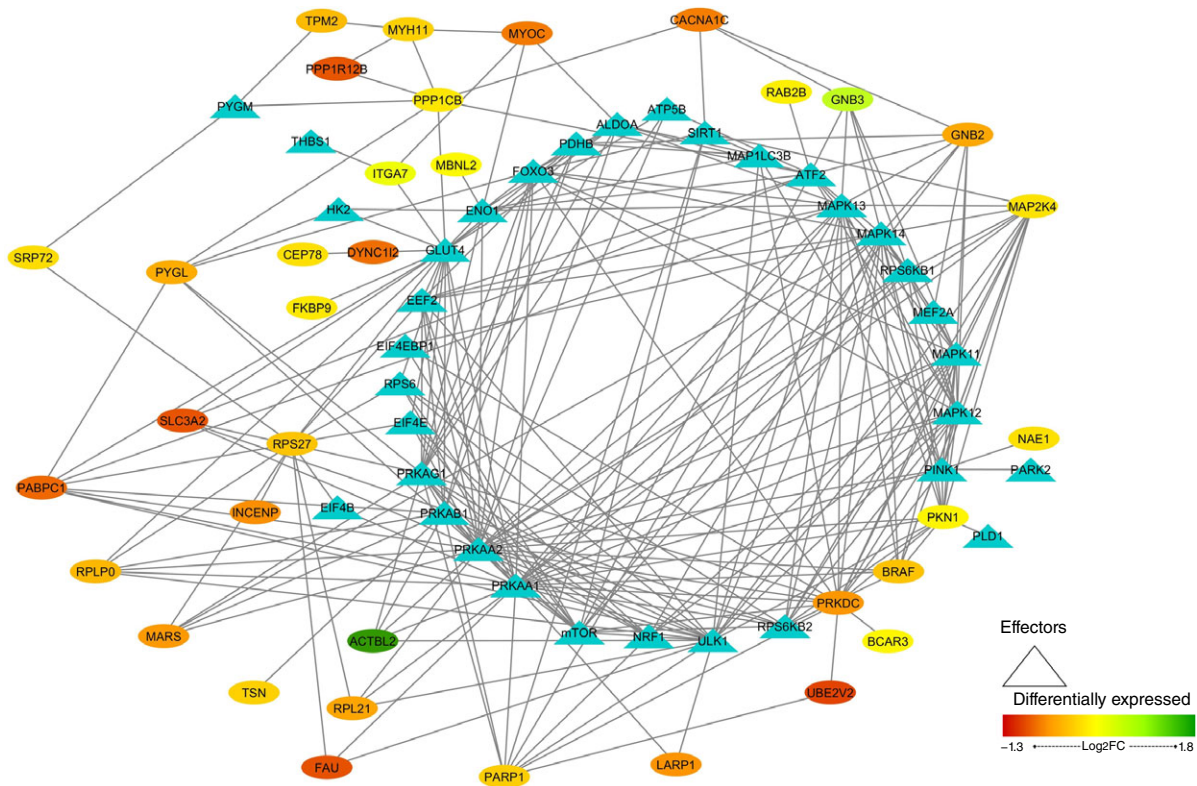
Figure 3. Visual protein interaction network of the proteins significantly related to skeletal muscle adaptations to endurance exercise training according to the artificial neuronal network score (ANNs), and their interacting proteins, in wild-type (*wt/wt*) mice
The network includes include three representations of the following interactions: (i) within the differentially expressed proteins (ovals), (ii) between the differentially expressed proteins and skeletal muscle adaptions to endurance exercise effectors (ovals and triangles), and (iii) within the skeletal muscle adaptations to endurance exercise effectors (triangles).

background, both LIMCH1 and PARP1 could participate in stress pathways controlled by exercise. Indeed, cell contraction accelerates when LIMCH1 promotes the assembly of actin stress fibres during cell spreading. Moreover, the absence of LIMCH1 expression impacts the formation of actin stress fibres as well as the stability of focal adhesions (Lin *et al.* 2017), which are fundamental structures in the union of muscle fibres to ensure optimal contraction and muscular distention. TIGD4 protein belongs to the tigger subfamily of the pogo superfamily of DNA-mediated transposons in humans. The latter proteins are related to DNA transposons found in fungi and nematodes and more distantly to transposases Tc1 and mariner, and they are very similar to the major mammalian B centromere protein. However, the exact function of TIGD4 remains to be clarified.

PARP1 is the most characterized member of the PARP family of nuclear enzymes. These proteins are sensitive to changes in intracellular redox pathways, positioning the poly ADP-ribosylation (PARylation) reaction as an important biochemical marker of oxidative stress (Jungmichel *et al.* 2013). Whereas basal activity of PARP1 is crucial to maintain cellular homeostasis, its over-activity leads to an increase in protein PARylation, which in turn depletes intracellular NAD^+ levels, leading to cell death (Ha & Snyder, 1999). Thus, PARP1 activity is a key sensor for cell survival. Interestingly, we found that endurance exercise training mediates the expression of PARP1 in both McArdle and wild-type mice, although it was higher in trained McArdle than in trained wild-type mice. This

could be due, at least partly, to high muscle damage that characterizes this disease.

In general, the low overlap between groups (74 and 123 differentially expressed proteins with training in wild-type and McArdle mice, respectively) suggests considerable differences in the physiological adaptations to chronic endurance exercise between McArdle and wild-type mice, at a mechanistic level. Indeed, when we compared the protein profile between McArdle and wild-type mice after training, we found that McArdle mice presented a specific and strong expression of MAPK12 and a potentially substantial number of effector interactions. MAPK12 is a serine/threonine kinase that acts as an essential component of the MAP kinase signal transduction pathway. Also known as p38MAPKγ, MAPK12 is one of the four p38 MAPKs that play an important role in the cellular response cascade induced by extracellular stimuli such as proinflammatory cytokines or physical stress (Cuenda & Rousseau, 2007). MAPK12 plays a role in myoblast differentiation, as it is involved in the regulation of the expression of the solute carrier family 2 (facilitated glucose transporter), member 1 (SLC2A1). Further, basal glucose uptake in L6 myotubes and MAPK12 signalling positively regulate the expansion of transient amplifying myogenic precursor cells during muscle growth and regeneration (Ho *et al.* 2004). Our analyses suggest that MAPK12 is also related to mitochondrial biogenesis and remodelling, with such potentially MAPK12-mediated improvement in mitochondrial function perhaps endeavouring to compensate for the deficit in energy supply
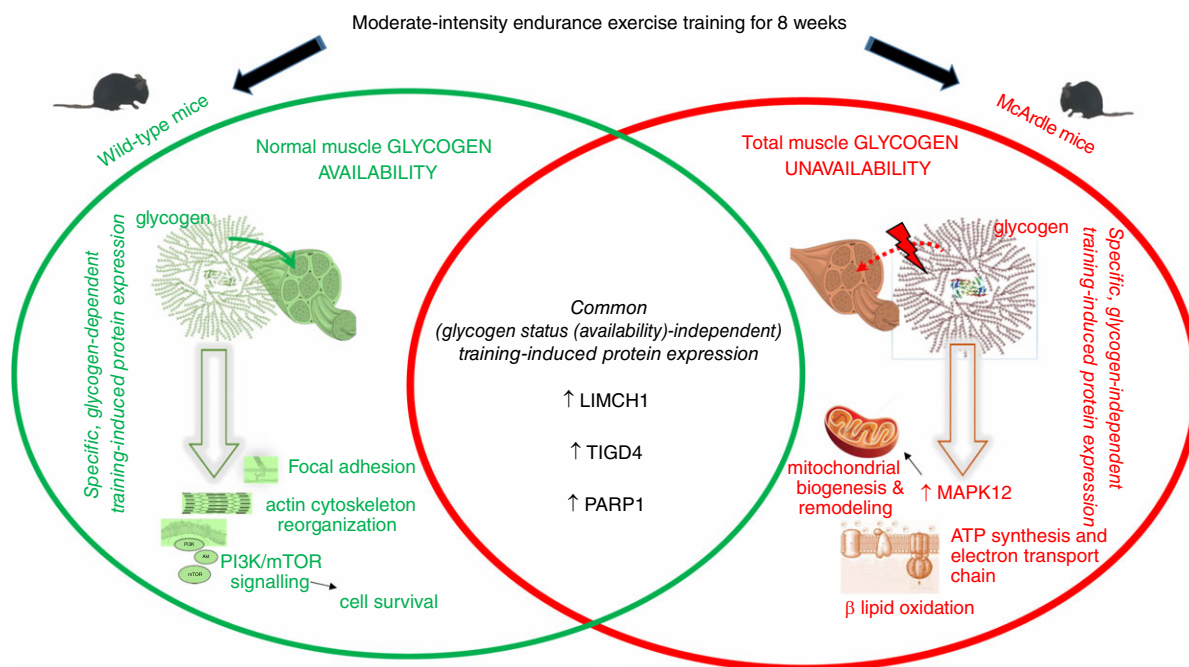

Figure 4. Integrative model summarizing the main study findings
Abbreviations: LIMCH1, LIM and calponin homology domains-containing protein 1; MAPK12, mitogen-activated protein kinase 12; PARP1, poly (ADP-ribose) polymerase 1; TIGD4, tigger transposable element derived 4.

owing to glycogen unavailability. By contrast, we detected a lower endurance exercise training-induced increase in MPAK12 protein expression in wild-type mice.

Pathway enrichment analysis of the highly and significantly expressed proteins in McArdle and wild-type mice (121 and 79 proteins, respectively) provided an enrichment in clinical processes that are related to the induction of oxidative stress, neuropathies and retinopathies. When McArdle and wild-type mice were analysed separately, we observed that after endurance exercise training in McArdle mice the most widely represented functions were those involved in ATP synthesis and electron transport chain processes, β-oxidation of lipids, and different steps in lipid and protein catabolism. In addition, cell death and regulation of necrotic processes were also reflected in this analysis. In fact, the overexpression of PARP1 could be associated with rhabdomyolysis, and PARP activation is linked to necrosis, as shown in PARP-deficient mouse fibroblasts (Ha & Snyder, 1999). All of the aforementioned adaptations found in McArdle mice after endurance exercise training may be related to the metabolic strategies that the skeletal muscle tissue of McArdle mice deploys to obtain energy. Conversely, after endurance exercise training the functions that were most represented in wild-type mice were those related to cytoskeleton regulation and focal adhesions, and also PI3K and mTOR signalling pathway activation related to maintenance of skeletal muscle cell survival. Thus, from an overall perspective, it seems that the main muscle molecular adaptations to endurance exercise training in McArdle mice are more oriented to obtain energy for tissue *regeneration* in a state of energetic deficit, whereas wild-type muscle adaptations seem to be more related to support tissue *maintenance* while coping with exercise stress stimuli.

Our study is not without limitations. In contrast to human research, where performing repeated muscle biopsy sampling may be feasible, a first technical limitation is the impossibility to determine muscle glycogen content before and after a training session in the wild-type mice as a proof-of-concept for glycogen utilization. Of note, owing to the total inability to utilize glycogen as a fuel, massive muscle glycogen accumulation occurs in McArdle mice, a phenomenon much more remarkable than in patients, with muscle glycogen levels being several orders of magnitude higher than in CB7Bl/6J wild-type mice as used here (Nogales-Gadea *et al.* 2012). Moreover, we chose forced treadmill running rather than wheel running as a model of endurance exercise training. Although wheel running is a less stressful, more natural form of activity in rodents, it does not allow for the establishment of predetermined training loads, which was a crucial aspect of our design to ensure they were similar in the exercise groups. Nevertheless, researchers in charge of mouse training were well experienced in mouse handling

such as to minimize stress in these animals. Indeed, only gentle tail touching was used to prompt the mice to run and no electrical stimulation was applied during the training sessions. Another potential limitation comes from the use of a single muscle type, quadriceps (with a highly glycolytic phenotype) for proteome analyses. Future research should determine whether comparable findings are obtained in a more oxidative muscle like the soleus or even in other glycolytic muscles. In this regard, although there are differences between muscles (even between those with a similar metabolic phenotype and with only subtle differences in proportion of fibre types, such as the quadriceps and tibialis anterior) overall, both fast- and slow-twitch muscles in the untrained state are affected by both structural degeneration and energy deficiency in McArdle mice (Krag *et al.* 2016*a*). Along this line, recent research has identified the quadriceps muscle as having more compensatory adaptations to counterbalance energetic deficiency in the untrained state (i.e. in terms of expression of proteins involved in glucose uptake, glycogen synthesis and glycolysis) than other studied muscles, whether they were predominantly glycolytic (tibialis anterior, extensor digitorum longus) or more oxidative (soleus) (Krag *et al.* 2016*b*). Finally, we did not report blood serum creatine kinase levels (as an indirect marker of muscle damage) over the study period.

In conclusion, we have determined that, akin to patients, McArdle mice responded favourably to moderate-intensity endurance exercise training, although their maximal aerobic capacity is clearly lower than that of normal peers. This suggests that glycogen availability is crucial for ensuring maximal endurance performance in mammals, with unavailability of this substrate resulting in muscles adopting a remarkably different 'molecular strategy' to cope with the training loads while ensuring cellular homeostasis during a state of energetic deficit. In this regard, we have identified for the first time the signalling strategies (in terms of signalling molecules and protein networks) that skeletal muscle employs to overcome blockade of glycogen breakdown during endurance exercise training, demonstrating that the protein network involved in muscle adaptations to such a type of training greatly differs depending on glycogen availability (see also Fig. 4 for a summary). Our findings provide a framework for future studies aimed at elucidating the molecular mechanisms associated with the most relevant identified proteins here. It would also be interesting to study in depth some of the proteins sets identified by the enrichment analysis; among which, PARP1, LIMCH1 and MAPK12 emerge as good candidates.

Appendix

Tables A1–A9.

Table A1. Molecular effectors of skeletal muscle adaptations to endurance exercise training determined through the review of specialized scientific literature

MOTIVE ID	Effector protein (name)	Effector protein (short name)
Adaptive muscle growth	40S ribosomal protein S6	RPS6 (rpS6)
	E3 ubiquitin-protein ligase TRIM63	TRIM63
	Elongation factor 2	EEF2
	Eukaryotic translation initiation factor 4B	IF4B
	Eukaryotic translation initiation factor 4E	EIF4E (eIF4E)
	Eukaryotic translation initiation factor 4E-binding protein 1	EIF4EBP1 (4EBP1)
	Forkhead box protein O3	FOXO3
	Growth/differentiation factor 8	MSTN
	Mechanistic target of rapamycin	mTOR
	Peroxisome proliferator-activated receptor γ coactivator 1-α	PGC-1α
	Phospholipase D1	PLD1
	Phospholipase D2	PLD2
	Ribosomal protein S6K 1	RPS6KB1 (p70S6K1)
	Ribosomal protein S6K 2	RPS6KB2 (p70S6K2)
Angiogenesis	Cyclic AMP-dependent transcription factor ATF-2	ATF2
	Mitogen-activated protein kinase 12	MAPK12 (p38g)
	Myocyte-specific enhancer factor 2A	MEF2A (MEF2)
	Nitric oxide synthase, endothelial	NOS3
	Peroxisome proliferator-activated receptor γ coactivator 1-α	PGC-1α
	Steroid hormone receptor ERR1	ESRRA (ERRa)
	Thrombospondin-1	TSP-1
	Vascular endothelial growth factor A	VEGFA
Glucose and lipid metabolism adaptations	α-Enolase	ENO1
	β-Enolase	ENO3
	Carnitine *O*-palmitoyltransferase 1, muscle isoform	CPT1B
	Fatty acid-binding protein, heart	FABP3 (FABPH)
	Glycogen phosphorylase, muscle form	PYGM
	Glyoxalase I (lactoylglutathione lyase)	GLO1
	Muscle form hexokinase	HK2
	Muscle-type aldolase	ALDOA
	Platelet glycoprotein 4	FAT/CD36
	Pyruvate dehydrogenase E1 component subunit α, somatic form, mitochondrial	PDHA1 (PDHa)
	Pyruvate dehydrogenase E1 component subunit β, mitochondrial	PDHB (PDHb)
	Solute carrier family 2, facilitated glucose transporter member 4	SLC2A4 (GLUT4)
Mitochondrial biogenesis and remodelling	5-Aminolevulinate synthase, non-specific, mitochondrial	ALAS1
	5′-AMP-activated protein kinase catalytic subunit α-1	PRKAA1 (AMPKa1)
	5′-AMP-activated protein kinase catalytic subunit α-2	PRKAA1 (AMPKa2)
	5′-AMP-activated protein kinase subunit β-1	PRKAB1 (AMPKb)
	5′-AMP-activated protein kinase subunit γ-1	PRKAG1 (AMPKg)
	ATP synthase subunit β, mitochondrial	ATP5B
	BCL2/adenovirus E1B 19 kDa protein-interacting protein 3	BNIP3
	BCL2/adenovirus E1B 19 kDa protein-interacting protein 3-like	BNIP3L
	Cyclic AMP-dependent transcription factor 2	ATF2
	Cytochrome *c* oxidase subunit 1	MT-CO1
	Cytochrome *c* oxidase subunit 2	MT-CO2
	Cytochrome *c* oxidase subunit 3	MT-CO3
	Cytochrome *c* oxidase subunit 4 isoform 1, mitochondrial	COX4I1
	Cytochrome *c* oxidase subunit 4 isoform 2, mitochondria	COX4I2
	Cytochrome *c* oxidase subunit 5A, mitochondrial	COX5A
	Cytochrome *c* oxidase subunit 5B, mitochondrial	COX5B

(Continued)

Table A1. Continued

MOTIVE ID	Effector protein (name)	Effector protein (short name)
	Cytochrome c oxidase subunit 6A1, mitochondrial	Cox6a1
	Cytochrome c oxidase subunit 6A2, mitochondrial	Cox6a2
	Cytochrome c oxidase subunit 6B1	Cox6b1
	Cytochrome c oxidase subunit 6B2	Cox6b2
	Cytochrome c oxidase subunit 6C	Cox6c
	Cytochrome c oxidase subunit 7A-related protein, mitochondrial	Cox7r
	Cytochrome c oxidase subunit 7A1, mitochondrial	Cox7a1
	Cytochrome c oxidase subunit 7A2, mitochondrial	Cox7a2
	Cytochrome c oxidase subunit 7B, mitochondrial	Cox7b
	Cytochrome c oxidase subunit 7C, mitochondrial	Cox7c
	Cytochrome c oxidase subunit 8A, mitochondrial P	Cox8a
	Cytochrome c oxidase subunit 8C, mitochondrial	Cox8c
	E3 ubiquitin-protein ligase parkin	PARK2 (PARKIN)
	FUN14 domain-containing protein 1	FUNDC1
	Microtubule-associated proteins 1A/1B light chain 3B	MAP1LC3B (LC3)
	Mitochondrial fission 1 protein	FIS1
	Mitofusin-1	MFN1
	Mitofusin-2	MFN2
	Mitogen-activated protein kinase 11	MAPK11 (p38b)
	Mitogen-activated protein kinase 12	MAPK12 (p38g)
	Mitogen-activated protein kinase 13	MAPK13 (p38d)
	Mitogen-activated protein kinase 14	MAPK14 (p38a)
	Myocyte-specific enhancer factor 2A	MEF2A (MEF2)
	NAD-dependent protein deacetylase sirtuin-1	SIRT1
	Nuclear respiratory factor 1	NRF-1
	Nuclear respiratory factor 2 (GA-binding protein subunit β-1)	NRF-2
	Peroxisome proliferator-activated receptor γ coactivator 1-α	PGC-1α
	PTEN-induced putative kinase protein 1	PINK1
	Putative cytochrome c oxidase subunit 7A3, mitochondrial	Cox7a3
	Serine/threonine-protein kinase ULK1	ULK1 (ATG1)
	Steroid hormone receptor ERR1	ESRRA (ERRa)
	Transcription factor A, mitochondrial	TFAM

Table A2. Summary of training loads in the two exercise groups (McArdle and wild-type) during the endurance exercise training programme

Training load variable	Week 1 (5 sessions)	Week 2 (5 sessions)	Week 3 (5 sessions)	Week 4 (5 sessions)	Week 5 (5 sessions)	Week 6 (5 sessions)	Week 7 (5 sessions)	Week 8 (3 sessions)
Intensity (%)*	55 (50, 60)	56 (50, 60)	61 (55, 65)	56 (50, 70)	59 (50, 65)	65 (55, 70)	66 (55, 75)	62 (50, 75)
Treadmill inclination (%)	0%	3 (0, 5)	9 (5, 15)	9 (5, 15)	13 (10, 15)	14 (10, 15)	14 (10, 15)	12 (5, 15)
Session duration (min)	32 (30, 35)	35 (30, 40)	41 (35, 45)	40 (40, 40)	43 (35, 50)	44 (35, 50)	45 (40, 50)	40 (30, 50)
Distance/session (McArdle, m)	227 (207, 255)	264 (219, 305)	328 (292, 364)	337 (324, 362)	341 (280, 386)	372 (349, 412)	389 (261, 462)	396 (219, 455)
Distance/session (wild-type, m)	303 (277, 344)	339 (283, 392)	423 (371, 473)	432 (385, 447)	440 (355, 492)	446 (434, 471)	463 (383, 481)	468 (411, 493)

Data are mean and range (min, max) for the core part of all the sessions within each week. *Determined as percentage of the velocity reached at the end of the maximal performance test performed at the start of the study (abbreviated as V_{max} in the text). Of note, training loads decreased in the two days of the 8th week (Wednesday and Thursday) that preceded the final performance test (Friday).

Table A3. List of the differentially expressed proteins between the trained and sedentary McArdle mice (*n* = 123) and the trained and sedentary wild-type mice (*n* = 74)

McArdle mice			Wild-type mice		
Mouse UniProt ID	Human Uniprot ID	Gene name	Mouse UniProt ID	Human Uniprot ID	Gene name
O08710	P01266	*TG*	P28028	P15056	*BRAF*
O08529	P17655	*CAPN2*	Q9QZK2	O75815	*BCAR3*
F6TQW2	—	—	B1ATL6	P45985	*MAP2K4*
Q8VCP8	Q9Y3D8	*AK6*	Q99LH9	Q7L8J4	*SH3BP5L*
Q5HZY7	O75348	*ATP6V1G1*	E0CXQ2	P0CG20	*PRR35*
Q9Z0P5	Q6IBS0	*TWF2*	Q3UK27	Q13564	*NAE1*
Q5SSW2	Q14997	*PSME4*	Q8BFZ3	Q562R1	*ACTBL2*
Q9DC11	Q6UX71	*PLXDC2*	Q9D404	Q9NWU1	*OXSM*
Q9JHU4	Q14204	*DYNC1H1*	O09167	P46778	*RPL21*
Q8CHH9	Q92599	*SEPT8*	Q920Q6	Q96DH6	*MSI2*
Q5RKZ7	Q9NZB8	*MOCS1*	P47802	Q13505	*MTX1*
Q545F5	P56381	*ATP5E*	Q54AE3	P16520	*GNB3*
P48774	P21266	*GSTM3*	P59279	Q8WUD1	*RAB2B*
P70670	E9PAV3	*NACA*	Q9WU62	Q9NQS7	*INCENP*
Q9Z0 × 1	O95831	*AIFM1*	P62880	P62879	*GNB2*
Q99LP6	Q9HAV7	*GRPEL1*	O08638	P35749	*MYH11*
D3YUB6	Q5XKL5	*BTBD8*	Q5M8R8	P05388	*RPLP0*
O08663	P50579	*METAP2*	Q9ET01	P06737	*PYGL*
Q61838	P20742	*PZP*	Q8BUZ3	Q8IY51	*TIGD4*
Q8C5W0	Q96JQ2	*CLMN*	Q8VHS6	Q8WXK1	*ASB15*
P01864	—	—	A2BFF7	Q13409	*DYNC1I2*
P01887	P61769	*B2M*	Q99K23	Q9NUQ7	*UFSP2*
Q3UX10	A6NHL2	*TUBAL3*	Q6ZQ58	Q6PKG0	*LARP1*
A0A0A6YW72	Q6V1P9	*DCHS2*	Q80 × 76	—	—
P08121	P02461	*COL3A1*	Q8BGF0	O00534	*VWA5A*
O88196	P53804	*TTC3*	O35206	P39059	*COL15A1*
P01837	P01834	*IGKC*	P21845	Q15661	*TPSAB1*
P97371	Q06323	*PSME1*	Q5XPI3	Q5XPI4	*RNF123*
Q4VAA2	Q9UKY7	*CDV3*	Q62348	Q15631	*TSN*
Q14C59	Q86T26	*TMPRSS11B*	Q9D2M8	Q15819	*UBE2V2*
Q921I1	P02787	*TF*	E9Q740	O76094	*SRP72*
Q9R1P0	P25789	*PSMA4*	Q9CQ89	O60888	*CUTA*
P05213	P68363	*TUBA1B*	E9PYH6	O15047	*SETD1A*
P84089	P84090	*ERH*	Q01815	Q13936	*CACNA1C*
Q3U1N0	P31146	*CORO1A*	Q8BL65	Q6H8Q1	*ABLIM2*
Q8R0Y8	Q86VD7	*SLC25A42*	P62862	P35544	*FAU*
Q5M9K7	P46783	*RPS10*	Q9D7 × 8	O75223	*GGCT*
Q9CQH7	Q96K17	*BTF3L4*	P28650	Q8N142	*ADSSL1*
Q8R404	Q5XKP0	*MIC13*	G3 × 9Q1	Q13683	*ITGA7*
O35857	O43615	*TIMM44*	P97822	Q9BTT0	*ANP32E*
P01867	—	—	A6H6K1	Q9BXN1	*ASPN*
Q9R0P9	P09936	*UCHL1*	P11103	P09874	*PARP1*
Q4VAE3	Q6PI78	*TMEM65*	Q60718	Q99965	*ADAM2*
Q6P549	O15357	*INPPL1*	P10852	P08195	*SLC3A2*
F6ZAP6	—	—	Q0VBD0	P26012	*ITGB8*
P62984	P62987	*UBA52*	P62141	P62140	*PPP1CB*
O09174	Q9UHK6	*AMACR*	P29341	P11940	*PABPC1*
E9PYB0	Q8IVF2	*AHNAK2*	Q8C4G9	Q86SQ6	*ADGRA1*
Q811B1	Q86Y38	*XYLT1*	Q8C0K5	P16260	*SLC25A16*
Q80ZW2	Q8WUY1	*THEM6*	Q3UH68	Q9UPQ0	*LIMCH1*
Q9D0F3	P49257	*LMAN1*	Q69ZX8	O94929	*ABLIM3*

(Continued)

Table A3. Continued

McArdle mice			Wild-type mice		
Mouse UniProt ID	Human Uniprot ID	Gene name	Mouse UniProt ID	Human Uniprot ID	Gene name
E9Q616	Q09666	*AHNAK*	P97313	P78527	*PRKDC*
Q9WUU7	Q9UBR2	*CTSZ*	P31786	P07108	*DBI*
P09103	P07237	*P4HB*	Q01339	P02749	*APOH*
P16015	P07451	*CA3*	Q8VED9	Q3ZCW2	*LGALSL*
O35593	O00487	*PSMD14*	Q6R0H7	O95467	*GNAS*
Q542A1	Q9UHQ4	*BCAP29*	A2AIM4	P07951	*TPM2*
Q9EQZ7	Q9UQ26	*RIMS2*	Q9CXJ4	Q9NUT2	*ABCB8*
Q9Z2C5	Q13496	*MTM1*	Q8C181	Q5VZF2	*MBNL2*
Q8R092	Q9BWL3	*C1orf43*	Q6ZWU9	P42677	*RPS27*
Q99J47	Q6IAN0	*DHRS7B*	Q9EPM5	Q9H7C4	*SYNC*
Q546G4	P02768	*ALB*	P70268	Q16512	*PKN1*
Q80ZS3	Q9BYN8	*MRPS26*	Q6IRU7	Q5JTW2	*CEP78*
P61222	P61221	*ABCE1*	Q8CHG3	Q8IWJ2	*GCC2*
Q8CI51	Q96HC4	*PDLIM5*	Q32NZ6	Q6UXY8	*TMC5*
A2AE45	—	—	Q1XH17	Q6ZMU5	*TRIM72*
Q9D1M0	P55735	*SEC13*	Q9Z247	O95302	*FKBP9*
Q99NB1	Q9NUB1	*ACSS1*	Q62205	Q15858	*SCN9A*
Q8BUZ3	Q8IY51	*TIGD4*	Q8BG95	O60237	*PPP1R12B*
Q62087	Q15166	*PON3*	B0QZF7	Q8NCQ7	*PROCA1*
O88492	Q96Q06	*PLIN4*	Q8BYH7	Q9HA65	*TBC1D17*
O55222	Q13418	*ILK*	P11627	P32004	*L1CAM*
Q3V1H3	Q6MZM0	*HEPHL1*	O70624	Q99972	*MYOC*
Q3U4U6	P49368	*CCT3*	E9QB02	P56192	*MARS*
Q9JIY5	O43464	*HTRA2*			
P06728	P06727	*APOA4*			
Q544H9	Q96T49	*PPP1R16B*			
P53986	P53985	*SLC16A1*			
A3KGG4	A7MBM2	*DISP2*			
Q61207	P07602	*PSAP*			
Q9JKF7	Q9NYK5	*MRPL39*			
P06330	—	—			
Q8R2Q4	Q969S9	*GFM2*			
Q9JK42	Q15119	*PDK2*			
Q9CR61	P17568	*NDUFB7*			
Q8CG76	O43488	*AKR7A2*			
Q6PB66	P42704	*LRPPRC*			
P50136	P12694	*BCKDHA*			
O08911	P53778	*MAPK12*			
Q1RLL3	Q8IYJ1	*CPNE9*			
Q8C2K5	Q86YV0	*RASAL3*			
Q80YR9	Q8IXT5	*RBM12B*			
Q4FJQ6	P35237	*SERPINB6*			
Q61001	O15230	*LAMA5*			
Q61187	Q99816	*TSG101*			
Q8K3C3	Q8WZA0	*LZIC*			
P06797	O60911	*CTSV*			
A2AAJ9	Q5VST9	*OBSCN*			
Q3UZA1	Q6JBY9	*RCSD1*			
Q99N13	Q9UKV0	*HDAC9*			
Q8BGK2	Q8NDY3	*ADPRHL1*			
P67778	P35232	*PHB*			
P17047	P13473	*LAMP2*			

(Continued)

Table A3. Continued

McArdle mice			Wild-type mice		
Mouse UniProt ID	Human Uniprot ID	Gene name	Mouse UniProt ID	Human Uniprot ID	Gene name
D3YX79	—	—			
Q8CII2	O75794	CDC123			
E9PV24	P02671	FGA			
P17427	O94973	AP2A2			
Q99L88	Q13884	SNTB1			
P11103	P09874	PARP1			
Q9JHL1	Q15599	SLC9A3R2			
Q3U2W2	Q9BQG0	MYBBP1A			
Q9WV96	Q9Y5J6	TIMM10B			
Q66JT0	P0C1S8	WEE2			
A2AKU9	P36542	ATP5C1			
A2AP31	O95139	NDUFB6			
P33173	Q12756	KIF1A			
Q921I2	Q8TBB5	KLHDC4			
Q8BTS4	Q7Z3B4	NUP54			
D3YU22	Q9UPQ0	LIMCH1			
Q61233	P13796	LCP1			
P22599	P01009	SERPINA1			
Q99MR8	Q96RQ3	MCCC1			
Q00623	P02647	APOA1			

Table A4. Number of proteins reported for each artificial neuronal network (ANN) category in relation to skeletal muscle adaptations to endurance exercise training in McArdle and wild-type mice; information is given for proteins individually ('individual'), in combination ('combined') and both ('total')

ANN category	McArdle						Wild-type						Common proteins
	Individual	%	Combined	%	Total	%	Individual	%	Combined	%	Total	%	
Strong ($P < 0.05$)	4	4%	135	2%	139	2%	0	0%	1	0%	1	0%	0
Medium–strong ($P = 0.05$–0.25)	29	25%	1900	34%	1 929	33%	16	22%	718	32%	734	31%	1
Weak ($P > 0.25$)	78	67%	3 636	64%	3 714	64%	52	71%	1 559	68%	1 611	69%	2
Not assessed	5	4%	0	0%	5	0%	5	7%	0	0%	5	0%	0
Total	116	100%	5 671	100%	5 787	100%	73	100%	2 278	100%	2 351	100%	3

Table A5. Summary of all the enriched protein sets (the corresponding database is also indicated)

Source	McArdle mice	Wild-type mice
BED	7	0
BED Motives	9	5
BED Pathways	5	3
GO Function	7	3
GO Location	35	1
GO Process	55	2
PharmGKB	2	1
TRRUST	1	0
KEGG	0	13
SMPDB	0	51
Total	121	79

Abbreviations: BED, Biological Effectors Database; GO, Gene Ontology; KEGG, Kyoto Encyclopedia of Genes and Genomes; PharmGKB, Pharmacogenomics Knowledgebase; SMPDB, Small Molecule Pathway Database; TRRUST, Transcriptional Regulatory Relationships Unraveled by Sentence-based Text-mining database.

Table A6. Enriched protein sets related to mitochondrial function in McArdle mice

Source	Set name
BED pathways	Oxidative phosphorylation (OXPHOS)
GO function ID	Proton-transporting ATP synthase activity, rotational mechanism
GO location	Mitochondrial crista junction
GO location	Mitochondrial inner membrane
GO location	Mitochondrial intermembrane space
GO location	Mitochondrial matrix
GO location	Mitochondrial proton-transporting ATP synthase complex
GO location	Mitochondrial proton-transporting ATP synthase complex, catalytic core F(1)
GO location	Mitochondrion
GO process	Mitochondrion organisation
GO process	Protein targeting to mitochondrion
GO process	Respiratory electron transport chain

Abbreviations: BED, Biological Effectors Database; GO, Gene Ontology;

Table A7. Enriched protein sets related to muscle structure and growth

Source	Set name
GO location	Costamere
GO location	Cytoskeleton
GO location	Focal adhesion
GO location	Membrane
GO location	Actin filament
GO process	Cell-matrix adhesion
GO process	Integrin-mediated signalling pathway
GO process	Positive regulation of Rho protein signal transduction
GO process	Regulation of actin cytoskeleton organization
GO process	Mitotic cell cycle
GO process	Positive regulation of ubiquitin-protein ligase activity involved in regulation of mitotic cell cycle transition
GO process	Regulation of ubiquitin-protein ligase activity involved in mitotic cell cycle

Abbreviations: GO, Gene Ontology.

Table A8. Summary of the enriched protein sets related to increase in muscle size and function, and neuromodulation

SOURCE	SET_NAME
KEGG	04510 _Focal adhesion
KEGG	04810 _Regulation of actin cytoskeleton
KEGG	04151 _PI3K-Akt signalling pathway
BED pathways	Gastrointestinal smooth muscle sustained contraction
BED pathways	Smooth muscle relaxation
BED pathways	Vascular smooth muscle contraction
KEGG	04270 _Vascular smooth muscle contraction
GO function	poly(U) RNA binding
GO function	Translation activator activity
GO process	Small GTPase mediated signal transduction
GO process	Translational initiation
KEGG	03015 _mRNA surveillance pathway
BED motives	Nervous impluse generation deffect
KEGG	04713 _Circadian entrainment
KEGG	04151 _PI3K-Akt signalling pathway
KEGG	04720 _Long-term potentiation
KEGG	04726 _Serotonergic synapse
KEGG	04727 _GABAergic synapse
KEGG	04728_Dopaminergic synapse

Abbreviations: BED, Biological Effectors Database; GO, Gene Ontology; KEGG, Kyoto Encyclopedia of Genes and Genomes.

Table A9. Summary of the enriched protein set related to catecholamine modulation within wild-type (*wt/wt*) mice; set sources are also indicated

Source	Set name	Source	Set name
PHARMKB	[PA2024] Beta-agonist/beta-blocker pathway, pharmacodynamics	SMPDB	[SMP00367] Carvedilol action pathway
SMPDB	[SMP00296] Acebutolol action pathway	SMPDB	[SMP00368] Labetalol action pathway
SMPDB	[SMP00297] Alprenolol action pathway	SMPDB	[SMP00375] Verapamil action pathway
SMPDB	[SMP00298] Atenolol action pathway	SMPDB	[SMP00376] Amlodipine action pathway
SMPDB	[SMP00299] Betaxolol action pathway	SMPDB	[SMP00377] Felodipine action pathway
SMPDB	[SMP00300] Bisoprolol action pathway	SMPDB	[SMP00378] Isradipine action pathway
SMPDB	[SMP00301] Esmolol action pathway	SMPDB	[SMP00379] Nifedipine action pathway
SMPDB	[SMP00302] Metoprolol action pathway	SMPDB	[SMP00380] Nimodipine action pathway
SMPDB	[SMP00303] Nadolol action pathway	SMPDB	[SMP00381] Nisoldipine action pathway
SMPDB	[SMP00304] Oxprenolol action pathway	SMPDB	[SMP00382] Nitrendipine action pathway
SMPDB	[SMP00305] Penbutolol action pathway	SMPDB	[SMP00588] Muscle/heart contraction
SMPDB	[SMP00306] Pindolol action pathway	SMPDB	[SMP00619] Felodipine metabolism pathway
SMPDB	[SMP00307] Propranolol action pathway	SMPDB	[SMP00657] Bopindolol action pathway
SMPDB	[SMP00320] Intracellular signalling through adenosine receptor A2a and adenosine	SMPDB	[SMP00658] Carteolol action pathway
SMPDB	[SMP00321] Intracellular signalling through adenosine receptor A2b and adenosine	SMPDB	[SMP00659] Timolol action pathway
SMPDB	[SMP00323] Quinidine action pathway	SMPDB	[SMP00660] Sotalol action pathway
SMPDB	[SMP00324] Procainamide (antiarrhythmic) action pathway	SMPDB	[SMP00661] Epinephrine action pathway
SMPDB	[SMP00325] Disopyramide action pathway	SMPDB	[SMP00662] Dobutamine action pathway
SMPDB	[SMP00326] Fosphenytoin (antiarrhythmic) action pathway	SMPDB	[SMP00663] Isoprenaline action pathway
SMPDB	[SMP00328] Lidocaine (antiarrhythmic) action	SMPDB	[SMP00664] Arbutamine action pathway
SMPDB	[SMP00329] Mexiletine action pathway	SMPDB	[SMP00665] Amiodarone action pathway
SMPDB	[SMP00330] Tocainide action pathway	SMPDB	[SMP00666] Levobunolol action pathway
SMPDB	[SMP00331] Flecainide action pathway	SMPDB	[SMP00667] Metipranolol action pathway
SMPDB	[SMP00332] Ibutilide action pathway	SMPDB	[SMP00668] Bevantolol action pathway
SMPDB	[SMP00359] Diltiazem action pathway	SMPDB	[SMP00669] Practolol action pathway
SMPDB	[SMP00366] Nebivolol action pathway	SMPDB	[SMP00670] Bupranolol action pathway

References

Altschul SF, Gish W, Miller W, Myers EW & Lipman DJ (1990). Basic local alignment search tool. *J Mol Biol* **215**, 403–410.

Ayala JE, Bracy DP, James FD, Julien BM, Wasserman DH & Drucker DJ (2009). The glucagon-like peptide-1 receptor regulates endogenous glucose production and muscle glucose uptake independent of its incretin action. *Endocrinology* **150**, 1155–1164.

Bartlett JD, Hawley JA & Morton JP (2015). Carbohydrate availability and exercise training adaptation: too much of a good thing? *Eur J Sport Sci* **15**, 3–12.

Bassel-Duby R & Olson EN (2006). Signaling pathways in skeletal muscle remodeling. *Annu Rev Biochem* **75**, 19–37.

Berenbaum MC (1989). What is synergy? *Pharmacol Rev* **41**, 93–141.

Bergstrom J, Hermansen L, Hultman E & Saltin B (1967). Diet, muscle glycogen and physical performance. *Acta Physiol Scand* **71**, 140–150.

Blake JA, Eppig JT, Kadin JA, Richardson JE, Smith CL, Bult CJ & the Mouse Genome Database Group (2017). Mouse Genome Database (MGD) – 2017: community knowledge resource for the laboratory mouse. *Nucleic Acids Res* **45**, D723–D729.

Bonzon-Kulichenko E, Garcia-Marques F, Trevisan-Herraz M & Vazquez J (2015). Revisiting peptide identification by high-accuracy mass spectrometry: problems associated with the use of narrow mass precursor windows. *J Proteome Res* **14**, 700–710.

Brull A, de Luna N, Blanco-Grau A, Lucia A, Martin MA, Arenas J, Marti R, Andreu AL & Pinos T (2015). Phenotype consequences of myophosphorylase dysfunction: insights from the McArdle mouse model. *J Physiol* **593**, 2693–2706.

Cardona M, Lopez JA, Serafin A, Rongvaux A, Inserte J, Garcia-Dorado D, Flavell R, Llovera M, Canas X, Vazquez J & Sanchis D (2015). Executioner caspase-3 and 7 deficiency reduces myocyte number in the developing mouse heart. *PLoS One* **10**, e0131411.

Cuenda A & Rousseau S (2007). p38 MAP-kinases pathway regulation, function and role in human diseases. *Biochim Biophys Acta* **1773**, 1358–1375.

Favier FB, Benoit H & Freyssenet D (2008). Cellular and molecular events controlling skeletal muscle mass in response to altered use. *Pflugers Arch* **456**, 587–600.

Fiuza-Luces C, Nogales-Gadea G, García-Consuegra I, Pareja-Galeano H, Rufián-Vázquez L, Pérez LM, Andreu AL, Arenas J, Martín MA, Pinós T, Lucia A & Morán M (2016). Muscle signaling in exercise intolerance: insights from the McArdle mouse model. *Med Sci Sports Exerc* **48**, 1448–1458.

Fiuza-Luces C, Soares-Miranda L, Gonzalez-Murillo A, Palacio JM, Colmenero I, Casco F, Melen GJ, Delmiro A, Moran M, Ramirez M & Lucia A (2013). Exercise benefits in chronic graft versus host disease: a murine model study. *Med Sci Sports Exerc* **45**, 1703–1711.

Frolkis A, Knox C, Lim E, Jewison T, Law V, Hau DD, Liu P, Gautam B, Ly S, Guo AC, Xia J, Liang Y, Shrivastava S & Wishart DS (2010). SMPDB: The Small Molecule Pathway Database. *Nucleic Acids Res* **38**, D480–D487.

Frontera WR & Ochala J (2015). Skeletal muscle: a brief review of structure and function. *Calcif Tissue Int* **96**, 183–195.

Garcia-Marques F, Trevisan-Herraz M, Martinez-Martinez S, Camafeita E, Jorge I, Lopez JA, Mendez-Barbero N, Mendez-Ferrer S, Del Pozo MA, Ibanez B, Andres V, Sanchez-Madrid F, Redondo JM, Bonzon-Kulichenko E & Vazquez J (2016). A novel systems-biology algorithm for the analysis of coordinated protein responses using quantitative proteomics. *Mol Cell Proteomics* **15**, 1740–1760.

Grundy D (2015). Principles and standards for reporting animal experiments in *The Journal of Physiology* and *Experimental Physiology*. *J Physiol* **593**, 2547–2549.

Ha HC & Snyder SH (1999). Poly(ADP-ribose) polymerase is a mediator of necrotic cell death by ATP depletion. *Proc Natl Acad Sci USA* **96**, 13978–13982.

Haller RG, Wyrick P, Taivassalo T & Vissing J (2006). Aerobic conditioning: an effective therapy in McArdle's disease. *Ann Neurol* **59**, 922–928.

Han H, Shim H, Shin D, Shim JE, Ko Y, Shin J, Kim H, Cho A, Kim E, Lee T, Kim H, Kim K, Yang S, Bae D, Yun A, Kim S, Kim CY, Cho HJ, Kang B, Shin S & Lee I (2015). TRRUST: a reference database of human transcriptional regulatory interactions. *Sci Rep* **5**, 11432.

Herrando-Grabulosa M, Mulet R, Pujol A, Mas JM, Navarro X, Aloy P, Coma M & Casas C (2016). Novel neuroprotective multicomponent therapy for amyotrophic lateral sclerosis designed by networked systems. *PLoS One* **11**, e0147626.

Ho RC, Alcazar O, Fujii N, Hirshman MF & Goodyear LJ (2004). p38gamma MAPK regulation of glucose transporter expression and glucose uptake in L6 myotubes and mouse skeletal muscle. *Am J Physiol Regul Integr Comp Physiol* **286**, R342–R349.

Hoydal MA, Wisloff U, Kemi OJ & Ellingsen O (2007). Running speed and maximal oxygen uptake in rats and mice: practical implications for exercise training. *Eur J Cardiovasc Prev Rehabil* **14**, 753–760.

Iborra-Egea O, Galvez-Monton C, Roura S, Perea-Gil I, Prat-Vidal C, Soler-Botija C & Bayes-Genis A (2017). Mechanisms of action of sacubitril/valsartan on cardiac remodeling: a systems biology approach. *NPJ Syst Biol Appl* **3**, 12.

Isern J, Martin-Antonio B, Ghazanfari R, Martin AM, Lopez JA, del Toro R, Sanchez-Aguilera A, Arranz L, Martin-Perez D, Suarez-Lledo M, Marin P, Van Pel M, Fibbe WE, Vazquez J, Scheding S, Urbano-Ispizua A & Mendez-Ferrer S (2013). Self-renewing human bone marrow mesenspheres promote hematopoietic stem cell expansion. *Cell Rep* **3**, 1714–1724.

Jungmichel S, Rosenthal F, Altmeyer M, Lukas J, Hottiger MO & Nielsen ML (2013). Proteome-wide identification of poly(ADP-ribosyl)ation targets in different genotoxic stress responses. *Mol Cell* **52**, 272–285.

Kanehisa M, Goto S, Sato Y, Kawashima M, Furumichi M & Tanabe M (2014). Data, information, knowledge and principle: back to metabolism in KEGG. *Nucleic Acids Res* **42**, D199–D205.

Koulmann N & Bigard AX (2006). Interaction between signalling pathways involved in skeletal muscle responses to endurance exercise. *Pflugers Arch* **452**, 125–139.

Krag TO, Pinos T, Nielsen TL, Brull A, Andreu AL & Vissing J (2016*a*). Differential muscle involvement in mice and humans affected by McArdle disease. *J Neuropathol Exp Neurol* **75**, 441–454.

Krag TO, Pinós T, Nielsen TL, Duran J, García-Rocha M, Andreu AL & Vissing J (2016*b*). Differential glucose metabolism in mice and humans affected by McArdle disease. *Am J Physiol Regul Integr Comp Physiol* **311**, R307–R314.

Lane SC, Camera DM, Lassiter DG, Areta JL, Bird SR, Yeo WK, Jeacocke NA, Krook A, Zierath JR, Burke LM & Hawley JA (2015). Effects of sleeping with reduced carbohydrate availability on acute training responses. *J Appl Physiol (1985)* **119**, 643–655.

Lin YH, Zhen YY, Chien KY, Lee IC, Lin WC, Chen MY & Pai LM (2017). LIMCH1 regulates nonmuscle myosin-II activity and suppresses cell migration. *Mol Biol Cell* **28**, 1054–1065.

Lucia A, Nogales-Gadea G, Perez M, Martin MA, Andreu AL & Arenas J (2008). McArdle disease: what do neurologists need to know? *Nat Clin Pract Neurol* **4**, 568–577.

Lucia A, Ruiz JR, Santalla A, Nogales-Gadea G, Rubio JC, Garcia-Consuegra I, Cabello A, Perez M, Teijeira S, Vieitez I, Navarro C, Arenas J, Martin MA & Andreu AL (2012). Genotypic and phenotypic features of McArdle disease: insights from the Spanish national registry. *J Neurol Neurosurg Psychiatry* **83**, 322–328.

Martinez-Bartolome S, Navarro P, Martin-Maroto F, Lopez-Ferrer D, Ramos-Fernandez A, Villar M, Garcia-Ruiz JP & Vazquez J (2008). Properties of average score distributions of SEQUEST: the probability ratio method. *Mol Cell Proteomics* **7**, 1135–1145.

Mate-Munoz JL, Moran M, Perez M, Chamorro-Vina C, Gomez-Gallego F, Santiago C, Chicharro L, Foster C, Nogales-Gadea G, Rubio JC, Andreu AL, Martin MA, Arenas J & Lucia A (2007). Favorable responses to acute and chronic exercise in McArdle patients. *Clin J Sport Med* **17**, 297–303.

Navarro P, Trevisan-Herraz M, Bonzon-Kulichenko E, Nunez E, Martinez-Acedo P, Perez-Hernandez D, Jorge I, Mesa R, Calvo E, Carrascal M, Hernaez ML, Garcia F, Barcena JA, Ashman K, Abian J, Gil C, Redondo JM & Vazquez J (2014). General statistical framework for quantitative proteomics by stable isotope labeling. *J Proteome Res* **13**, 1234–1247.

Navarro P & Vazquez J (2009). A refined method to calculate false discovery rates for peptide identification using decoy databases. *J Proteome Res* **8**, 1792–1796.

Nogales-Gadea G, Pinos T, Lucia A, Arenas J, Camara Y, Brull A, de Luna N, Martin MA, Garcia-Arumi E, Marti R & Andreu AL (2012). Knock-in mice for the R50X mutation in the PYGM gene present with McArdle disease. *Brain* **135**, 2048–2057.

Pache RA, Zanzoni A, Naval J, Mas JM & Aloy P (2008). Towards a molecular characterisation of pathological pathways. *FEBS Lett* **582**, 1259–1265.

Pernow B & Saltin B (1971). Availability of substrates and capacity for prolonged heavy exercise in man. *J Appl Physiol* **31**, 416–422.

Rivals I, Personnaz L, Taing L & Potier MC (2007). Enrichment or depletion of a GO category within a class of genes: which test? *Bioinformatics* **23**, 401–407.

Russell AP (2010). Molecular regulation of skeletal muscle mass. *Clin Exp Pharmacol Physiol* **37**, 378–384.

Santalla A, Nogales-Gadea G, Ortenblad N, Brull A, de Luna N, Pinos T & Lucia A (2014). McArdle disease: a unique study model in sports medicine. *Sports Med* **44**, 1531–1544.

Sonnhammer EL & Ostlund G (2015). InParanoid 8: orthology analysis between 273 proteomes, mostly eukaryotic. *Nucleic Acids Res* **43**, D234–D239.

The UniProt Consortium (2017). UniProt: the universal protein knowledgebase. *Nucleic Acids Res* **45**, D158–D169.

Turk WR, Heller SL, Norris BJ & Nemeth PM (1990). Increased muscular β-hydroxyacyl CoA dehydrogenase with McArdle's disease. *Muscle Nerve* **13**, 607–612.

Vissing J & Haller RG (2003). The effect of oral sucrose on exercise tolerance in patients with McArdle's disease. *N Engl J Med* **349**, 2503–2509.

Webster CC, Noakes TD, Chacko SK, Swart J, Kohn TA & Smith JA (2016). Gluconeogenesis during endurance exercise in cyclists habituated to a long-term low carbohydrate high-fat diet. *J Physiol* **594**, 4389–4405.

Whirl-Carrillo M, McDonagh EM, Hebert JM, Gong L, Sangkuhl K, Thorn CF, Altman RB & Klein TE (2012). Pharmacogenomics knowledge for personalized medicine. *Clin Pharmacol Ther* **92**, 414–417.

Additional information

Competing interests

All the authors declare they have no conflict of interesting.

Author contributions

The experiments were performed in the Centre of Energy, Environment and Technical Research, CIEMAT (mouse genotyping, housing and training); and Centro Nacional de Investigaciones (Cardiovasculares): proteomics. C.F.L.: conception and design of the work, acquisition, analysis and interpretation of data for the work, and drafting the work; A.S.L. and J.L.Z.: design of the work, analysis and interpretation of data for the work, and drafting the work; F.L., J.A., M.A.M., A.L.A., T.P., B.G.B. and J.V.: interpretation of data for the work and revising the work critically for important intellectual content; G.N.G., J.D.B., R.C. and A.G.M.: acquisition of data for the work and revising the work critically for important intellectual content; C.B.: analysis and interpretation of data for the work and revising the work critically for important intellectual content; J.A.L.: analysis and interpretation of data for the work and revising the work critically for important intellectual content; A.L.: conception and design of the work, analysis and interpretation of data for the work, drafting the work. All authors qualify for authorship, approved the final version of the manuscript and agree to be accountable for all aspects of the work in ensuring that questions related to the accuracy or integrity of any part of the work are appropriately investigated and resolved.